Newsletter of the Climate Variability and Predictability Programme (CLIVAR)

Exchanges

No 47 (Volume 13 No 4) October 2008

From Heuser et al., page 20; Numerical Simulations of the Role of Land Surface Conditions on the Climate of Mt. Kilimanjaro Region

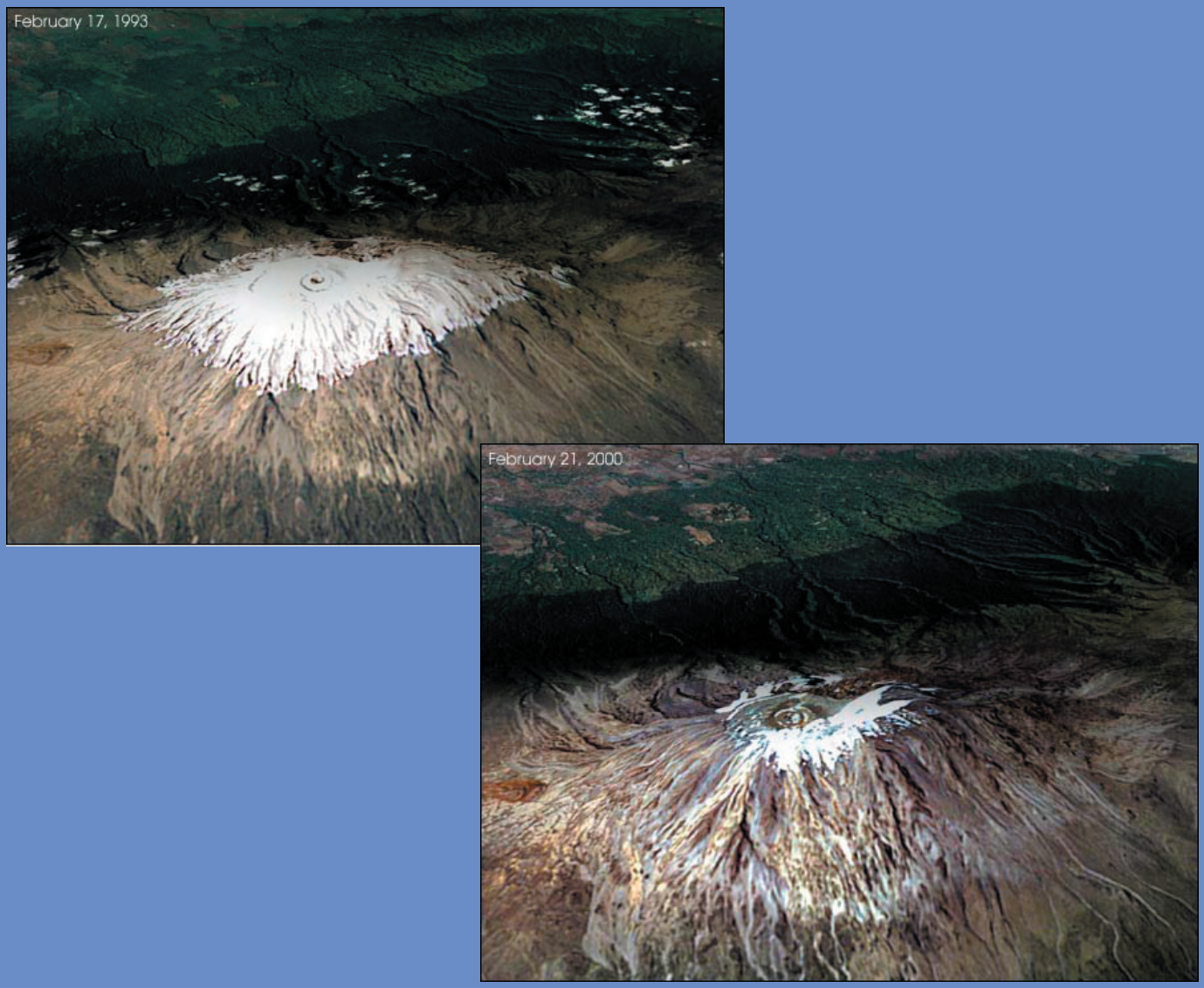

Figure 1: Kilimanjaro Ice Extent: February 1993 and February 2001

CLIVAR is an international research programme dealing with climate variability and predictability on time-scales from months to centuries. CLIVAR is a component of the World Climate Research Programme (WCRP). WCRP is sponsored by the World Meteorological Organization, the International Council for Science and the Intergovernmental Oceanographic Commission of UNESCO.

WCRP World Climate Research Programme

CALL FOR CONTRIBUTIONS

We would like to invite the CLIVAR community to submit CLIVAR related papers to CLIVAR Exchanges for the next issue. The deadline for submission is 30th November 2008

Guidelines for the submission of papers for CLIVAR Exchanges can be found under: http//www.clivar.org/publications/exchanges/guidel.php

Editorial

WCRP is considering its future. Hence, a key issue discussed by the Joint Scientific Committee (JSC) for WCRP when it met in Arcachon, France, last April was how to evolve the structure of WCRP to meet changing science priorities and societal needs and how to transition the work undertaken by the WCRP projects (CliC, CLIVAR, GEWEX and SPARC) to meet the challenges of the 21st century. The programme's evolution is seen as taking place on two time horizons – firstly to 2013 (the approximate previously declared "sunset dates" of the projects) and secondly into the next decade beyond. Consequently, all four of the WCRP core projects and the WCRP Working Groups have been asked to contribute to (a) developing a near-term "implementation" plan for WCRP against the priorities set out in the WCRP Strategic Plan 2005-2015 (subtitled "Coordinated Observation and Prediction of the Earth System", COPES [http://wcrp.ipsl.jussieu.fr]); (b) the development of an "accomplishments" document setting out WCRP's achievements for presentation, for example, at the upcoming World Climate Conference-3 (WCC-3) and other climate fora and (c) identifying how WCRP should evolve in the longer-term, beyond the 2013 timeframe.

To gather in the needed views and inputs, CLIVAR together with the other components of WCRP, has been asked to prepare a response to a number of detailed questions including:

1. *What will be the key science issues your project aims to address over the coming years, to 2013?*
2. *What elements of this science do you see as needing to be taken forward beyond thet?*
3. *What new science do you see WCRP needing to address beyond 2013 in the context of your project?*
4. *How is your project addressing the unifying cross-cutting foci of WCRP*
5. *What will be the major key legacy items of your project by 2001, and beyond?*

CLIVAR is addressing these requests by asking its panels and working groups to identify what they see as the "imperatives" and "frontiers of research on climate variability and predictability and the research infrastructure needed to support them". At the same time the ICPO is developing a draft response to the detailed questions from the JSC and which the panel responses will feed into. The resulting document will then be made available for community comment and further input before sending it to the JSC early in the New Year. Further subsequent community discussions can be expected, refining the document for CLIVAR's input to JSC-30 when it meets in Baltimore in April 2009. Outcomes of JSC-30 and the way forward for CLIVAR science will provide the focus for the discussions at CLIVAR SSG-16 in May. Overall this activity is a key opportunity for the CLIVAR community to influence the future of WCRP and its structure, to the benefit of international coordination of climate science. I hope to report on progress in future issues of "Exchanges".

This edition of Exchanges contains papers on various aspects of CLIVAR science demonstrating it's breadth. We welcome further such inputs for future editions (see front cover). In addition, I would be pleased indeed to receive community requests for further "themed" editions such as we have had in the past.

Howard Cattle

The Third Argo Science Workshop:

The Future of Argo

Call for Papers and Registration

25, 26 and 27 March 2009
Hangzhou, China

Talks and posters are invited on any topic based on substantial use of Argo data. The purpose of the workshop is to assess the scientific and wider utility of Argo and to consider the future evolution of the Argo program.

The deadline for abstract submissions is 19 December 2008, the deadline for registration is 23 January 2009.

For further information visit the meeting web site: www.argo.ucsd.edu/ASW3.html

Sponsored by the Argo Steering Team and PICES, the N. Pacific Marine Science Organization.

The Southwest PacIfic Ocean Circulation and Climate Experiment (SPICE): a new CLIVAR programme

Ganachaud, A.[1], W. Kessler[2], G. Brassington[3], C. R. Mechoso[4], S. Wijffels[5], K. Ridgway[5], W. Cai[6], N. Holbrook[7,8], P. Sutton[9], M. Bowen[9], B. Qiu[10], A. Timmermann[10], D. Roemmich[11], J. Sprintall[11], D. Neelin[4], B. Lintner[4], H. Diamond[12], S. Cravatte[13], L. Gourdeau[1], P. Eastwood[14], T. Aung[15]

[1]Laboratoire d'Etudes en Géophysique et Océanographie Spatiales (LEGOS)/Institut de Recherche pour le Développement (IRD), Nouméa, New Caledoni; [2]National Oceanic and Atmospheric Administration (NOAA)/Pacific Marine Environmental; Laboratory (PMEL), Seattle, WA, USA; [3]Centre for Australian Weather and Climate Research, A partnership between the Australian; Bureau of Meteorology and CSIRO, Melbourne, Australia, 3001; [4]Department of Atmospheric Sciences, University of California, Los Angeles, CA, USA; [5]CSIRO Marine and Atmospheric Research, Hobart, Australia; [6]CSIRO Marine and Atmospheric Research, Aspendale, Australia; [7]School of Geography and Environmental Studies, University of Tasmania, Hobart, Tasmania, Australia; [8]Centre for Marine Science, University of Tasmania, Hobart; Tasmania, Australia; [9]NIWA, Wellington, New Zealand; [10]University of Hawaii, Honolulu, HI, USA; [11]Scripps Institution of Oceanography, San Diego, CA, USA; [12]NOAA/National Climatic Data Center, Silver Spring, Maryland, USA; [13]Laboratoire d'Etudes en Géophysique et Océanographie Spatiales (LEGOS)/Institut de Recherche pour le Développement (IRD), Toulouse, France; [14]SOPAC, Suva, Fiji Islands; [15]USP, Suva, Fiji Islands.
Corresponding author: Alexandre.Ganachaud@noumea.ird.nc

Abstract

The Southwest Pacific is a region of complex oceanic and atmospheric circulation, with strong currents interacting with islands and the erratic behaviour of the South Pacific Convergence Zone (SPCZ), whose position and intensity modulate the wind field, heat flux and precipitation. To understand the circulation and its influence on local and remote climate, ocean and atmosphere scientists from Australia, France, New Zealand, the United States and Pacific Island countries initiated an international research project, the Southwest Pacific Ocean Circulation and Climate Experiment (SPICE). The project, endorsed by CLIVAR (http://www.clivar.org/organization/pacific/pacific_SPICE.php), reflects a strong sense that substantial progress will be made through collaboration among South Pacific national research groups, coordinated with broader South Pacific projects including VOCALS (VAMOS Ocean-Cloud-Atmosphere-Land Study; VAMOS = Variability of the American Monsoon Systems), NPOCE (Northwestern Pacific Ocean Circulation Experiment), and the developing PACSWIN (PACific Source Water Investigation). SPICE is purposely oriented towards long term monitoring to serve climate prediction, and to foster projects and collaborations with other fields such as ocean and weather forecasts, coral reef and ecosystem monitoring, and climate-related diseases. Here we present the outline of a regionally-coordinated experiment to model, measure, and monitor the ocean circulation and the SPCZ, to validate and improve numerical models, and to integrate with ocean/atmosphere data assimilating systems. Additionally SPICE will actively seek new collaborations with other research groups studying South Pacific climate variability.

1. Introduction

South Pacific thermocline waters are transported in the westward-flowing South Equatorial Current from the subtropical gyre center towards the southwest Pacific Ocean - a major circulation pathway that redistributes water from the subtropics to the equator and to the Southern Ocean (Figure 1). The transit of these thermocline waters in the Coral Sea is potentially important to tropical climate prediction because changes in either the temperature or the amount of water arriving at the equator can modulate the western warm pool and equatorial undercurrent. This has potential influence on the El Niño-Southern Oscillation (ENSO) cycle and subsequent basin-scale climate feedbacks as well as the Indonesian throughflow and the Indian Ocean. The southern pathway of thermocline waters is, comparably, of major influence on Australia and New Zealand's climate as its seasonal and inter-annual evolution influences air-sea heat flux and atmospheric conditions. Substantial changes of this circulation have been observed in recent years: the subtropical gyre has been spinning up with possible consequences for ENSO and for the East Australian Current (EAC) whose influence has moved south, dramatically affecting the climate and biodiversity of Tasmania.

Few observations are available to diagnose the processes and water pathways through the complicated geography of the numerous islands and ridges of the southwest Pacific (Figure 2). The South Pacific Convergence Zone (SPCZ) is poorly documented; access to many areas is difficult for conventional research platforms, and the large temporal variability and strong narrow currents in a region of complex bathymetry pose serious challenges to an observing system. Numerical model results are sensitive to parameter choices and forcing, and the value of such simulations remains uncertain because of the lack of in situ data for validation. The existing observational network (Argo, eXpandable Bathy Thermograph (XBT) sampling from voluntary observing ships, and satellite sea surface temperature, wind and sea surface height) is starting to provide a large-scale picture, but the complex circulation and strong western boundary currents require a thorough, dedicated, study.

Exploratory cruises in the Coral Sea occurred mainly from the mid 1950's to the mid 1980's (except for an intensive survey during World War II), however with the increased focus of research on El Niño associated with the TOGA programme, most of the attention (and funding, for almost 20 years) was devoted to the equatorial processes. In 2005, a small workshop was organized in the Queensland Tablelands, Australia, to review the current knowledge in

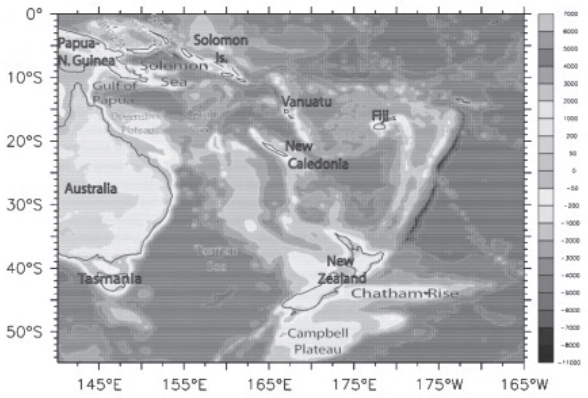

Figure 1: Geography and topography of the southwest Pacific. The incoming, westward flowing South Equatorial Current encounters large topographic obstacles before reaching the western boundaries.

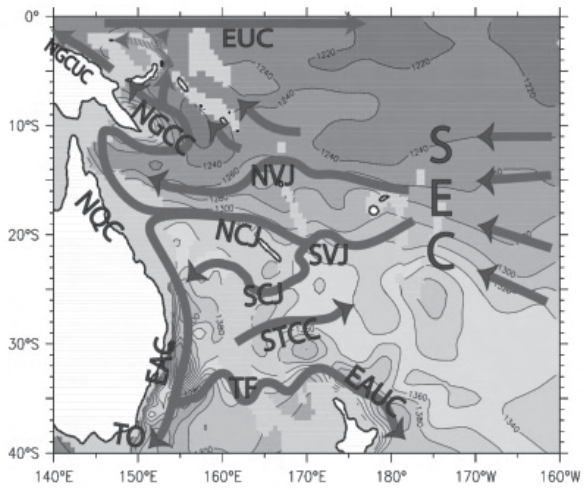

Figure 2: Integral dynamic height between 0 and 2000m (m^3/s^2) from the CSIRO Atlas of Regional Seas (CARS) data. Overlain are the major current systems of the Southwest Pacific. Complex pathways divide the southern part of the South Equatorial Current (SEC) into jets : North/South Vanuatu Jet (NVJ/SVJ), and South/North Caledonian Jet (NCJ/SCJ). Those jets feed the western boundary current system: the North Queensland Current (NQC) and New Guinea Coastal (Under) Current (NGCC/NGCUC), and, to the south, the East Australian Current (EAC). The northern fate of the water is the Equatorial Undercurrent (EUC) through the Solomon Straits. The southern fate is the Subtropical Countercurrent (STCC), the Tasman Front (TF) and the East Auckland Current (EAUC), and the Tasman Outflow (TO) to the south.

the area and envisage further exploration. Twenty-seven scientists met for 3 days and laid down the foundations of an international, regionally-coordinated experiment, the Southwest Pacific Ocean Circulation and Climate Experiment (SPICE).

The goal of SPICE is to observe, simulate and understand the role of the southwest Pacific Ocean circulation in (a) the large-scale, low-frequency modulation of climate from the Tasman Sea to the equator, and (b) the generation of local climate signatures. To achieve this, four specific efforts are proposed:

1. Analysis of the role of the southwest Pacific in global coupled models;
2. Development of an observational program to survey air-sea fluxes and currents in the Coral, Solomon and Tasman Seas, and their inflows and outflows, with special attention to the strong boundary currents and jets;
3. Combination of these observations with focused modeling efforts to devise a sustained monitoring program to adequately sample the time-variability of the currents and their heat and mass transports;
4. Use of remotely and locally sampled meteorological fields, and ocean model analysis, to determine the air-sea heat and freshwater fluxes and water mass transformations that occur in the region, and their effects on the local and global climate. A focus here may be the design of a process study to observe, model and understand the South Pacific Convergence Zone.

2. Organization

SPICE is regionally focused, but integrates basin-scale studies of the ocean-atmosphere system. The large-scale context including the basin-scale South Pacific circulation and its connection with equatorial processes and climate variability is addressed within CLIVAR and related projects. SPICE is organized in the following work areas (Figure 3):

- South Pacific Convergence Zone: formation, variability, air-sea interactions;
- South Equatorial Current inflow: jet formation, bifurcation against Australia, western boundary currents;
- Tasman Sea circulation: EAC/EAUC variability; heat balance and air-sea fluxes in the Tasman Sea;
- Gulf of Papua and Solomon Sea circulation: western boundary current and interior pathways, flow through the Solomon Straits;
- Downscaling and environmental impacts of climate and oceanic environment changes: cyclones; sea level rise; coral reef sustainability; coastal ecosystems.

The proposed approach is collaborative and cost-effective, based on existing manpower and technical resources. It will rely heavily on ocean and atmosphere modeling, combined with process studies to acquire basic knowledge in the north Coral Sea region; but also with monitoring where necessary and regional adaptation of global observing programs.

3. Modeling strategy

The SPICE program is stimulated by the need to improve climate prediction at both large and regional scales to allow island communities to benefit from climate research. Model experiments will provide the necessary linkage between large scale questions (e.g. how the subtropical gyre waters get to the Equator) and regional issues (e.g. what are the detailed oceanic pathways and impacts in the SW Pacific) through downscaling. Use of a variety of numerical models (Figure 4), validated against observations, will help to improve our understanding of the dynamical aspects that cannot be adequately observed and to identify the observable features thereby providing guidance to the design of the in-situ observing program. Model types range from global, coupled systems to local, high-resolution nested models (Figure 4, middle). Three existing operational oceanography projects are important for the Southwest Pacific (e.g., Bluelink, MERCATOR and SODA). The former two are assimilating systems that offer a nowcast and forecast estimate of the

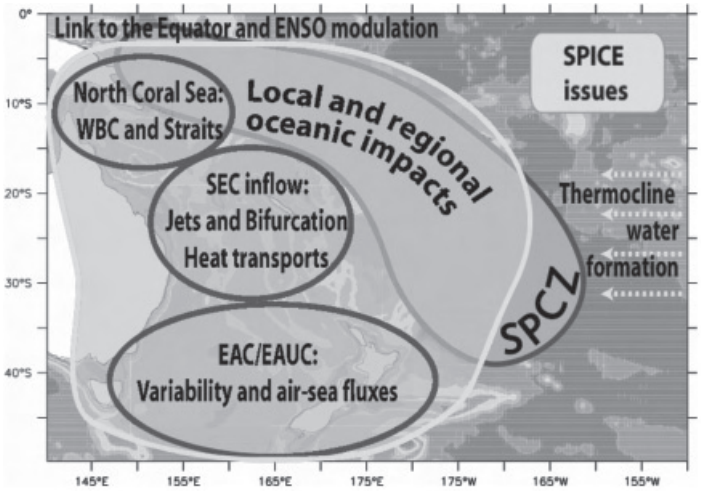

Figure 3: Main issues addressed within SPICE. The programme is regionally focused, but integrates larger scale programmes within CLIVAR (e.g. ENSO modulation). It is organized in four geographical areas with specific approaches, and favors interactions with regional studies specific to the different islands and coasts.

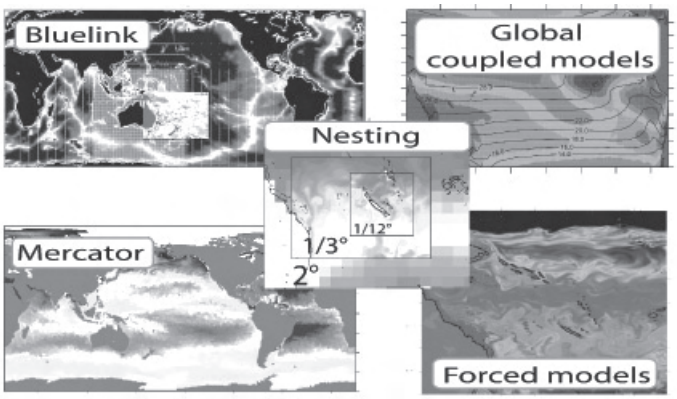

Figure 4: The modeling approach will rely on a range of models from coarse climate models to high-resolution, nested regional models. Upper left : the Bluelink (www.marine.csiro.au/bluelink) operational ocean model grid and southwest Pacific subdomain. Lower left: the Mercator French operational model (www.mercator-ocean.fr). Middle: nesting of the Noumea ROMS model from the 2° MERCATOR grid to 1/12° grid around New Caledonia (www.ird.nc/UR65/ROMS). Upper right: an IPCC-IR4 global coupled model. Lower right: the OFES high resolution ocean model.

true state of oceanic currents, temperatures and salinities which are supported operationally providing information throughout the SPICE experiment.

Modeling experiments will have to address a number of issues, such as understanding the oceanic and atmospheric teleconnections between the southwest Pacific and the basin-scale dynamics; the SPCZ formation process; key aspects of the thermocline water pathways (jet formation; bifurcation against the Australian coast; flow through the Solomon Sea; route to the Equator; variability along the East Australian Current and the Tasman Outflow); local ocean-atmosphere variability and impacts on the oceanic environment over the area.

Numerical simulations will be designed in order to improve the realism of the Southwest Pacific area in large-scale models. In particular the models will be used to improve our understanding of Southwest Pacific variability and its relation with basin-scale climate; to help design optimal observations; to simulate the small spatial scale features associated with boundary currents, islands and straits; to understand ocean-atmosphere interactions at island and coastal scales and to adapt, or downscale, global climate projections into results that are useful to island communities. Models will also be developed based on low-cost infrastructure so that participating countries can create or use their own modeling capacities.

The backbone of the SPICE modeling activities is the availability of regional expertise and computing facilities in four research centers (Melbourne, Wellington, Noumea and Hawaii), as well as SPCZ-modeling expertise at the University of California, Los Angeles. We propose to address the aforementioned issues using a variety of models and interlaced approaches. Six types of model will be used: 1) basin-scale general circulation models (GCMs) with a typical horizontal resolution ranging from 20 km - 200 km; 2) coupled GCMs; ocean data-assimilating: 3) ocean re-analyses and 4) operational GCMs; 5) regional (nested) models with a typical resolution of 2 km - 20 km and 6) process, or simplified, models. This approach will not only help to test and improve the IPCC projections in the Southwest Pacific, but will also help responding to a high demand for climate change forecasts from Pacific Island Countries which are the most vulnerable to changes in oceanic and atmospheric conditions. Overall, regional models are expected to help identify large scale model deficiencies and prompt their correction. Such improvement may be implemented through "upscaling", by embedding a regional model in a large scale model during integration or by improved parameterizations.

4. In situ observations

Analogous to high resolution models nested in global circulation models, the detailed regional SPICE measurements will complement large-scale observational programs, focusing on local aspects which are either un-resolved or under-resolved. Satellite ocean observations are mostly inadequate to observe the small scale variability and / or subsurface flows of interest. The Argo array provides temperature and salinity profiles over the top 2 km of the water column; however the Coral and Tasman seas are still little sampled by Argo. As a result, most of our knowledge of the hydrography and circulation in the Coral Sea comes from numerical models and climatologies based on sparse data. The observational database in the Tasman Sea is larger, however the high regional variability calls for targeted process experiments and monitoring. While investigations and further analysis of large-scale climatologies will be necessary, a substantial observational effort is needed in the Coral, Tasman and Solomon seas. A major SPCZ-focused field programme has also been envisaged during the design of SPICE, but given the present state of knowledge, it was decided to give priority to numerical model and analytical approaches complemented with analysis of remote sensing data and reanalysis products, without precluding a future SPCZ field experiment (AGU session - OS41B-0537 - SPICE: South PacIfic Circulation and Climate Experiment; December 2007).

The goal of the SPICE field program is to measure and monitor key, climate-relevant quantities. The proposed observations will include large-scale surveys of the Coral, Solomon and Tasman Sea inflows and outflows with special attention to the western boundary currents. A main focus of the observational program will be to test and apply large-scale, in-situ, and remote monitoring of key climate quantities, of which air-sea fluxes, SEC inflow, Solomon and Tasman Sea inflows and outflows are deemed critical. One of the major aims of the project is to close the regional mass, heat and freshwater budgets and to address local site-specific variations.

The field programme includes a variety of observations utilizing the most recent technological developments (e.g. use of gliders) and long-established XBT lines (Figure 5). The observational strategy was designed to address the issues of air-sea fluxes; SEC inflow / mass and heat transports entering the Coral Sea; jet characteristics; transports entering and exiting the Solomon Sea and a basic description of the circulation within the Solomon Sea; Tasman Sea inflows and outflows; and East Australian Current variability. These measurements will benefit studies of regional features and ocean environmental impacts (coastal circulation; water properties and coral reef health), and in some cases stimulate specific, simultaneous local observations based on common platforms.

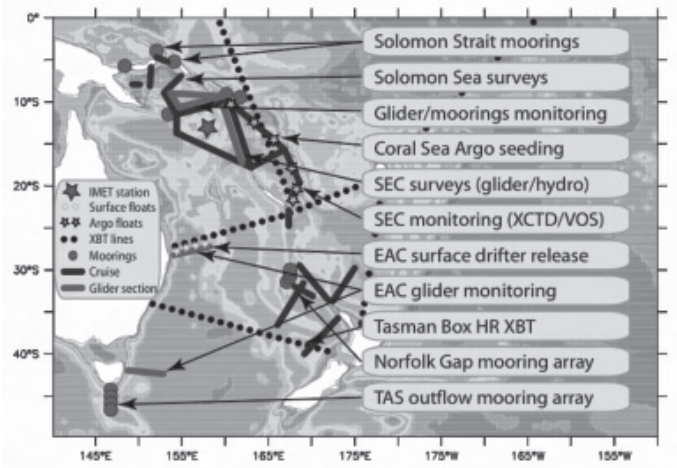

Figure 5: SPICE field experiment. Simultaneous measurements in different parts of the basin will allow analysis and monitoring of the mass/heat budget within the area. Exploratory surveys, some of which have already taken place, are followed by experimental monitoring, with a possible long term monitoring outcome. The different components are either planned, submitted, funded or completed. Fieldwork activities, excluding long term monitoring, are expected to last until 2012.

Although many aspects of the observational plan will be determined by targeted, regional projects, the broad outline is clear. It will rely on extensive regional collaboration, on the existing infrastructures and teams, and on regionally-focused adaptation of global observation programs. An important aspect will be the requirement for quasi-simultaneous observations in different parts of the basin. Exploratory surveys will be needed to identify key quantities that require monitoring (e.g. influx into the Solomon Sea). Experimental monitoring will be followed with the design of a long-term monitoring system at key locations. This in-situ observation plan will be completed with remote observations (e.g. sea surface temperature, height and salinity), calibrated and adapted regionally.

5. Data management and policy

Through the CLIVAR data policy (http://www.clivar.org/data/data_policy.php), measurements and model outputs pertaining to SPICE should be made publicly available through appropriate data servers. Relevant training will help building capacity in local communities to use southwest Pacific data and forecasts in pertinent response to societal demand.

6. Applications and training

The bridge between the large scale ocean and atmosphere circulation and their local impacts on environment and eventually societal sustainability will be established in collaboration with regional agencies and universities. On basin and global scales, the ultimate purpose of SPICE and follow-up projects is to improve climate prediction. Such improvement will be of direct benefit to Pacific Island Countries (PICs) whose climate is strongly influenced by ENSO. In addition, a major SPICE objective is to improve knowledge and prediction of the ocean conditions in the southwest Pacific, over a wide range of time scales and from basin to island space scales. Tools will be developed (e.g. database access; model simulation diagnostics), as well as self-contained projects that are specific to a location or process. This development, along with easy public data access, should align with appropriate training to serve local interests and respond to the demand from Pacific Island countries to improve their appreciation of vulnerability to changes in the oceanic and atmospheric environment as well as their capacity to respond to such changes.

SPICE in collaboration with the Pacific Islands Global Ocean Observing System (PI-GOOS, hosted by SOPAC, the Pacific Islands Applied Geoscience Commission, based in Suva, Fiji), will endorse training initiatives. Training can cover a wide range of topics, some of which are already mentioned in this document (e.g. sea level rise; oceanic conditions and coral reef health; tropical cyclones). Specific research or application projects are also encouraged with the potential for classes on database usage and the opportunity to develop regional expertise on operational oceanography

7. SPICE legacy

The efficacy and reliability of the proposed measurements on climate prediction will be assessed through the modeling efforts. This will pinpoint to the key quantities that may lead to the development of a long term South Pacific monitoring system and to deliver data for initialization and calibration of climate forecasts. Regionally, SPICE will lead to improved understanding of the ocean circulation and ocean forecasts, with direct applications to Pacific Island countries.

Key References (an extensive list can be found in the first two CLIVAR reports):

SPICE. Ganachaud, A., W. Kessler, S. Wijffels, K.Ridgway, W. Cai, N. Holbrook, M. Bowen, P. Sutton, B. Qiu, A. Timmermann, D. Roemmich, J. Sprintall, S. Cravatte, L. Gourdeau, and T. Aung., 2007. Southwest Pacific Ocean Circulation and Climate Experiment. Part I. Scientific Background. NOAA OAR Special Report / International CLIVAR Project Office, *CLIVAR Publication Series No. 111*

SPICE. Ganachaud, A., G. Brassington, W. Kessler, C. R. Mechoso, S. Wijffels, K.Ridgway, W. Cai, N. Holbrook, P. Sutton, M. Bowen, B. Qiu, A. Timmermann, D. Roemmich, J. Sprintall, D. Neelin, B. Lintner, H. Diamond, S. Cravatte, L. Gourdeau, P. Eastwood and T. Aung., 2008 Southwest Pacific Ocean Circulation and Climate Experiment. Part II. Implementation plan. *CLIVAR report* (in press ; http://www.clivar.org/organization/pacific/pacific_SPICE.php)

SPCZ: Takahashi, K., and D. S. Battisti, 2007 : Processes Controlling the Mean Tropical Pacific Precipitation Pattern. Part II: The SPCZ and the Southeast Pacific Dry Zone. *J. Clim*. **20**, 5696-5706.

Lintner, B. R. and J. D. Neelin, 2008: Eastern margin variability of the South Pacific Convergence Zone. *GRL* **35**, L16701, doi:10.1029/2008GL034298

Operational: Schiller, A. et al., 2008: Eddy-resolving ocean circulation in the Asian–Australian region inferred from an ocean reanalysis effort. *Progress Oceanogr*., **76** 334–365

General circulation:

Ridgway, K. and J. Dunn, 2003. Mesoscale structure of the East Australian Current System and its relationship with topography. *Progress in Oceanography*, **56**, 189 – 222.

Gliders and jets. Gourdeau, L., W. Kessler, R. Davis, J. Sherman, C. Maes and E. Kestenare (2008). "Zonal jets entering the Coral sea." *J. Phys.Oceanogr.* **38**: 715-725.

Dynamics. Holbrook, N.J. and N.L. Bindoff, 1999: Seasonal temperature variability in the upper southwest Pacific Ocean. *J. Phys. Oceanogr*., **29**, 366-381;

Kessler, W. and L. Gourdeau (2007). "The annual cycle of circulation of the southwest subtropical Pacific, analyzed in an ocean GCM." *J. Phys. Oceanogr*. **37**: 1610-1627.

Evaluation of water masses in ocean syntheses products

Gemmell, A.L., G. C. Smith, K. Haines, J. D. Blower
Environmental Systems Science Centre, University of Reading, UK
Corresponding author: alg@mail.nerc-essc.ac.uk

Ocean syntheses are an important tool for understanding interannual-to-decadal ocean climate variability by combining ocean observations with general circulation models to provide a time-evolving state of the ocean. Such syntheses have been used, for example, in studies of oceanic heat content (Carton and Santorelli 2008, Kohl *et al.*, 2007), sea level variability, Wunsch *et al.* 2007, and for reconstructing the Atlantic meridional overturning circulation (Wunsch and Heimbach, 2006; Balmaseda *et al.*, 2007). A number of different syntheses have been produced, which vary considerably in model formulation and resolution, as well as the methods and data-types used in the assimilation process. Under the auspices of the CLIVAR Global Synthesis and Observations Panel (GSOP), an intercomparison is underway to better understand the differences and applicability of the various syntheses to climate relevant questions. Herein, we present ongoing work as part of the GSOP intercomparison into the water mass properties of the various synthesis products. Information on other intercomparisons is available from www.clivar.org/data/synthesis/directory.php

The volume and temperature/salinity (T/S) properties of ocean water masses are key diagnostics for surveys of the world oceans such as WOCE (Siedler *et al.* 2001) and, unlike circulation and transports, are accessible to direct hydrographic sampling. The advent of the complete Argo array (Gould; 2005) in 2007 provides a near-continuous sampling of water mass properties of the upper 2 km of the global ocean, allowing us survey for the first time how well ocean synthesis products compare and to identify their differences.

Product	Assimilation
FOAM 1°	OI Operational
ECMWF 1° (ORA3)	OI Operational
INGV 2° (to 2001)	OI
CERFACS 2° (to 2001)	3DVar
ECCO-GODAE 1°	4DVar
ECCO-JPL 1°	KF-Smoother
ECCO-SIO 1° (to 2001)	4DVar
GECCO 1° (to 2001)	4DVar
SODA ¼°	OI
Mercator ¼° (2007 on)	OI Operational
Reading DRAKKAR 1°	OI
Reading DRAKKAR ¼°	OI
WOA05 1°	Climatology

Table 1. Model/synthesis/reanalysis datasets with metadata currently stored in OceanDIVA. Products are monthly means unless otherwise noted. In addition to the products in the table, observations can also be compared to the World Ocean Atlas 2005 gridded 1° climatology.

As these syntheses are spread over a number of OPeNDAP servers, a new tool called OceanDIVA (www.resc.rdg.ac.uk/OceanDIVA_info.php) has been developed at the Reading e-Science Centre to collect and intercompare these datasets. OceanDIVA reads a collection of hydrographic profiles, y, and gridded model synthesis data (from the remote servers), x, and interpolates the gridded model products in space and time, to determine the model equivalent of the observation profiles, i.e. the Observation Operator H(x). Nearest neighbour grid points are used in the horizontal plane, while in the vertical, linear interpolation to depth (z) or temperature (T) can be selected to define a coordinate, with T(z), S(z) or z(T), S(T) being evaluated by the observation operator, as well as model-data misfits, H(x)-y. Output is then generated in either KMZ format (zipped KML) for viewing the profiles in Google Earth (coloured by various misfits or profile types), or as shown here, as regional probability density functions (PDFs) of the model-data misfits.

Here we present results using all available Argo and XBT profiles for a single month (September 2004), which consists of approximately 10,000 profiles globally (of which 5700 include salinity data), to provide a baseline against which to compare misfits from the different GSOP ocean synthesis products listed in Table 1; mostly a subset of those listed on www.clivar.org/data/synthesis/directory.php. We focus here on comparisons for the North Pacific, however, comparisons for other regions may be found both in the supplementary material to be found at http://www.clivar.org/publications/exchanges/extra/47/and in Gemmell *et al.* (2008).

Figure 1 (page 13) shows examples of how water mass errors appear in these probability plots, using the gridded WOA05 data (Boyer *et al.*; 2006) as a reference. Figure 1a shows the z(T) PDF of observed values for profiles from September 2004 in the North Pacific (30°N – 70°N and 100°W- 100°E). The colours indicate the probability of a particular depth being observed for a particular temperature surface (with warmer colours indicating a greater probability). The presence of sub-tropical mode water (STMW) can be seen in the large amount of 17°C water with depths between 200-400m. The PDF for T(z) observations would look similar just turned clockwise by 90°, but the equivalent misfit plots look quite different. Figures 1b and 1d show the profile misfits against the WOA05 climatology, for z(T) and T(z) respectively. The North Pacific mode waters, poorly captured in WOA05, now show up very clearly in the z(T) misfits as a large depth error localized around 17°C. In contrast, these errors are not discernable in the T(z) misfits (Figure. 1d) as the errors occur over a range of depths resulting in the signal being too spread out. The nature of this error can be seen in Figure 1c, which shows a typical pair of profiles contributing to these PDF misfits from the Google Earth display. The observed profile shows clearly the mode water as a fairly homogenous layer with uniform temperatures between 200-400m while the WOA05 profile smoothes this out entirely thereby contributing to the z(T) error at 17°C seen in the PDF.

Figures 2a and 2b (page 13) show z(T) and S(T) misfits respectively, for the North Pacific against the same September 2004 profile data, for 10 different ocean synthesis products (Table 1). Six of the products are from low resolution models (~1°), 3 of which use sequential assimilation (FOAM, ECMWF-ORA3 and Reading 1°), 2 use a long-window 4DVar approach (ECCO-GODAE and GECCO) and ECCO-JPL is a Kalman-filter-smoother. Four of the products are from high resolution ¼° models: SODA, Mercator (Sep 07), Reading¼, and the Reading¼ control run (otherwise known as DRAKKAR-G70, Barnier *et al.*; 2007).

The z(T) error in subtropical mode waters discussed in Figure 1 for WOA05, is present to varying degrees in the different synthesis products (Figure 2a). The SODA and Reading¼ high resolution products have perhaps the smallest mode water misfits, both having considerably smaller errors than WOA05 (Figure 1b). Some other products show a small shallow bias in mode water depths (e.g. Reading1 and ECMWF) while others have both deep and shallow errors equally. Looking now at the whole temperature range, it is remarkable that the 4DVar synthesis products (ECCO-GODAE and GECCO), and the Kalman Filter product ECCO-JPL, have rather similar bias errors in z(T) to the Reading¼ control run (similarities also occur in S(T) misfits in Figure 2b discussed below). In particular, waters cooler than 7°C are too deep, suggesting perhaps a downward diffusion of temperature, coupled with a lack of cold deep water formation.

Where Figure 2a focused on vertical water mass positions (i.e. z(T) distributions), Figure 2b shows the water mass property errors (S(T) misfits). The biases and error spread in water mass distributions between the different products is clearly illustrated. The Reading¼ control run and the ECCO products both have positive salinity biases for intermediate water temperatures between 5-15°C, of up to 0.25psu at around 7.5°C. This is the same temperature range in which the waters are too deep in Figure 2a, and is consistent with downward diffusion of saline waters and a lack of renewal of deep fresher waters. A similar pattern of large biases is also present in other ocean basins (see supplementary material).

It should be remembered that most of these synthesis products are assimilating the same, or a very similar set, of profile data to those they are being compared with, so the results reflect the degree to which the assimilation has constrained these aspects of the synthesis, i.e. z(T) and S(T). It should also be noted that a number of products (GECCO, INGV and CERFACS) are disadvantaged because they represent September 2001 rather than September 2004, as this was the latest synthesised data available. Therefore interannual errors will increase their misfits against 2004 observations, as will their reduced exposure to any Argo data. The Mercator product is only available for September 2007 and so will have interannual errors, but it has assimilated good Argo data which should remove biases.

These products are all based on quite different numerical models although there will be similarities in the atmospheric forcing. The sequential data assimilation schemes introduce data directly into the models (through non-conservative fluxes of heat and mass) and most produce fairly tight and unbiased S(T) relationships. The long window 4DVar methods that constrain the syntheses less tightly to in situ observations, such as those of the ECCO project, seem less able to correct or maintain unbiased water mass properties over periods of years to decades. Despite the ability of 4DVar to adjust surface forcing to bring the synthesis in better agreement with observations, the resulting water mass properties clearly have similar biases to the uncontrained Reading control run. The ECCO-JPL result also appears have similar large water mass errors and therefore the constraints to in situ observations cannot be strong.

In order to summarise information in Figure 2a,b for a wide range of synthesis products on a single diagram, we plot the mean and standard deviation misfits for intermediate waters between 5°C and 15°C in the North Pacific, on orthogonal axes (with the total RMS misfits contoured as distances from the origin) for all products (Figure 3, page 14). Note that the mean and standard deviation of misfits among the different products tend to increase together for both the water mass properties, S(T), and the isotherm geometry, z(T). As such, unbiased synthesis products are more likely to have smaller random errors. In addition, products with smaller S(T) misfits also have smaller z(T) misfits. As might be expected, the sequential assimilation systems have the smallest mean and standard deviation errors, with several outperforming the WOA05 climatology product. Synthesis products from September 2001 (filled symbols) have larger bias and standard deviations than most products from September 2004. The temporal differences can be cleanly assessed for the Reading 1° product which is shown for both times.

The effect of model resolution and assimilation can be seen in Figure 3 by comparing the four Reading products. By increasing the resolution from 1° to ¼°, the RMS misfits in the control runs are reduced for both S(T) and z(T). However, when observed profiles are assimilated into these models then a much larger reduction in both mean and standard deviation of misfits occurs, reducing the RMS error to less than that of the WOA05 climatology.

This diagnostic can also be used to summarise the subtropical mode water differences in the North Pacific. Figure 4a (page 14) shows clearly how the high-resolution products with sequential assimilation (Reading¼ and SODA) provide the tightest fit to the observations. Other products have a larger degree of scatter due to a combination of factors related to the numerical model and assimilation methods used. Alternatively this diagnostic can be expanded to summarise the whole globe. Figure 4b shows the S(T) misfits for the whole globe for waters 5-15°C. Many of the biases and misfits seen in Figure 2b and summarised in Figure 3a for the North Pacific, related to model resolution and assimilation method, are also seen in other basins. The synthesis results for the global domain in Figure 4b therefore show a similar ordering to Figure 3a.

These figures produced by the OceanDIVA tool allow a very rapid assessment of many synthesis products using different water mass based measures of the misfit errors. This has allowed us to understand and quantify the range of water mass properties in the synthesis products to help understand the nature of the differences and their sources. This tool is freely available to the scientific community via the Reading e-Science Centre website (www.resc.rdg.ac.uk) and may be used for particular regional studies, or to analyse other synthesis products available on any OPeNDAP server.

References

Balmaseda, M. A., G.C. Smith, K. Haines, D. Anderson, T.N. Palmer and A. Vidard (2007): Historical reconstruction of the Atlantic meridional overturning circulation from ECMWF operational ocean reanalysis. *Geophys. Res. Lett.*, **34**, L23615, doi:10.1029/2007GL031645.

Barnier, B. *et al.*, (The DRAKKAR Group), 2007: Eddy-permitting Ocean Circulation Hindcasts Of Past Decades. *CLIVAR Exchanges*, **12(3)**, 8-10.

Boyer T. P., J. I. Antonov, H. E. Garcia, D. R. Johnson, R. A. Locarnini, A. V. Mishonov, M. T. Pitcher, O. K. Baranova and I. V. Smolyar, 2006: World Ocean Database 2005. in S. Levitus, Ed., NOAA Atlas NESDIS 60, U.S. Government Printing Office, Washington, D.C., 190 pp., DVDs.

Carton, J.A. and A. Santorelli 2008 Global decadal upper ocean heat content as viewed in nine analyses, *Submitted to J. Climate.*

Gemmell A.L., G.C. Smith, K. Haines and J.D. Blower 2008: Validation of ocean model syntheses against hydrography using a new web application. *Submitted to J. Operational Oceanography.*

Gould, J., 2005: From swallow floats to Argo—The development of neutrally buoyant floats. *Deep Sea Res.*, **52**, 529–543.

Köhl, A., D. Stammer, and B. Cornuelle, 2007: Interannual to Decadal Changes in the ECCO Global Synthesis. *J. Phys. Oceanogr.*, **37**, 313–337.

Siedler G., J. Church and J. Gould (Eds) 2001: Ocean circulation and climate: modelling and observing the global ocean. Academic Press, 715pp.

Wunsch, C., and P. Heimbach, 2006: Estimated Decadal Changes in the North Atlantic Meridional Overturning Circulation and Heat Flux 1993–2004. *J. Phys. Oceanogr.*, **36**, 2012–2024.

Wunsch, C., R.M. Ponte, and P. Heimbach, 2007: Decadal Trends in Sea Level Patterns: 1993–2004. *J. Climate*, **20**, 5889–5911

On isothermal diagnostics of ocean heat content

Haines, K[1]., and M. D. Palmer[2]
[1]Environmental Systems Science Centre, University of Reading, United Kingdom. [2]Met Office Hadley Centre, United Kingdom.
Corresponding author: kh@mail.nerc-essc.ac.uk

Changes in ocean heat content (OHC) should provide the clearest indication of the extent to which the Earth has been a net absorber of solar radiation due to changing greenhouse gas concentrations. Ocean warming measurements have played an important role in the Intergovernmental Panel on Climate Change (IPCC) AR4 assessment process (Bindoff *et al*. 2007), and the detailed characteristics of the signals have also been used for detection and attribution of anthropogenic effects in climate models (Barnett *et al*., 2005; Pierce *et al*., 2006). However the record of subsurface ocean temperature changes is very incomplete in space and time (e.g., Harrison and Carson, 2006), and is heavily subject to calibration of the observing platforms, such as Expendable Bathythermograph (XBT) bias errors which have come to light recently (Domingues *et al*., 2008; Wijffels *et al*., 2008). The oceans are also subject to decadal change due to low frequency climate forcing modes such as the North Atlantic Oscillation (NAO) and the Pacific Decadal Oscillation (PDO), which cause large changes in local heat content through changing advection patterns, which can alias into basin and global scale trends when combined with a historically sparse observing array (Palmer *et al*., 2007). These factors all lead to uncertainty in ocean heat content estimation.

Our study is a reassessment of the historical ocean temperature profile measurements and attempts to separate the influence of surface heat fluxes from the advective convergence components of local heat content change, by recording both the depth of isotherms D, and the mean temperature of the water above isotherms <T>. Conventional heat content would measure mean temperature of water down to a fixed depth H only. Palmer *et al*., (2007) have already shown that global trends in the mean temperature above the 14°C isotherm show a more uniform spatial distribution than fixed depth measurements. If OHC = $C_p\rho_0 H[T]$, where C_p is the specific heat capacity, ρ_0 the mean background density and [T] is the average temperature to the fixed depth H, we now define relative heat content (RHC), at some time =t, as;

$$RHC_t = C_p \rho_0 D_t \left(\langle T_t \rangle - T_{ref} \right) \quad (1)$$

where T_{ref} is the reference isotherm at depth D_t and <> is the average down to depth D_t. For small changes in time we can write;

$$RHC_t \approx \rho C_p \left(\langle T \rangle' \overline{D} + D' \left(\overline{\langle T \rangle} - T_{ref} \right) \right) \quad (2)$$

where overbars are time means and primes are temporal anomalies. Now RHC changes can be attributed to isotherm deepening D', or to warming of the whole water column <T>'.

The 7.4 million quality controlled temperature (T) profiles from the European Union (EU) ENACT (ENhAnced ocean data assimilation and ClimaTe prediction) project are used, covering 1956-2004, as described in Ingleby and Huddleston (2007). All profile data are binned monthly on a regular 2° grid, and a seasonal climatology is produced, along with monthly anomalies over the 49 years, for all quantities required. Figure 1 (page 14) shows the change between decades 1965-74 and 1995-04 in the OHC, the RHC, and the two components of RHC, as defined in Eq 2, with T_{ref} = 14°C, and H=220m, the global mean depth of T_{ref}.

The patterns of OHC and RHC change are very similar in nearly all basins (correlation = 0.74), although with greater RHC increase in the North Atlantic due to the deeper thermocline there. The mean temperature component of RHC change, reflecting mainly surface induced warming (correlated 0.57 with OHC), is more uniform, while the depth change component (also correlated 0.57 with OHC) has more variability and has strong signals in the subtropical gyres of the N. Atlantic and N. Pacific which have the characteristic imprint of NAO, (Visbeck *et al*., 2003) and PDO (e.g. Parker *et al*., 2007) forcing changes. [Correlations of RHC with <T>' and D' are 0.67 and 0.84, respectively, i.e. depth changes dominate spatial variability.]

Basin	Trends 1970-2000 = Equivalent surface forcing (Wm^{-2})			
	OHC	RHC	RHC-<T>′	RHC-D′
Globe	0.09	0.15	0.14	0.02
Atlantic	0.36	0.52	0.32	0.22
Pacific	-0.04	0.0	0.06	-0.07
Indian	0.08	0.06	0.09	-0.02

Table 1: Equivalent time-mean surface heating (Wm^{-2}) for the period 1970-2000, based on trends in the time series.

Figure 2 shows smoothed time series of global and basin integrated anomalies for OHC, RHC and its 2 components, and Table 1 gives trends based on these time series. There is no infilling so the time series reflect anomalies only in the areas sampled each month. The time series of OHC and RHC show similar temporal evolution, with greatest differences in the Atlantic Ocean where the 14°C isotherm shows the largest deviations from the 220m fixed depth surface. Trends are calculated from 1970 onwards when the time series are more robust due to better (equipment or spatial/temporal coverage?) sampling. The upward RHC trend in the Indian basin is almost entirely due to mean temperature changes. In the Pacific there is little total trend due to a cancellation of mean warming with a shoaling of isotherms. Only the Atlantic has a large RHC trend due to deepening, and this reflects the dominant sampling in the N. Atlantic subtropical gyre. There is a mean temperature increase in all basins consistent with the greater uniformity in Figure 1c, and the global RHC trend is dominated by this warming. The deepening contribution to the RHC trend in the Atlantic appears to cancel with the shoaling trend in the Pacific and Indian oceans, consistent with the advective redistribution of warmer waters. One detail worth noting in Figure 2 is that the impact of volcanic aerosols shows up clearly in the mean temperature contribution, especially in the Indian Ocean, but there is little sign of aerosol induced anomalies from the depth contributions to RHC.

Palmer *et al*., (2007) discuss the heaving in the depth of isotherms due to both high (wave/Ekman), and low (Ekman) frequency advective convergence of upper ocean waters. The mean temperature above isotherms is little affected by such dynamics and this is reflected in reduced high and low frequency variance in the mean temperature contribution to RHC (see Palmer and Haines, 2008; and also Figure 2). They also point out that XBT fall rate errors only affect isotherm depth and not mean temperature above isotherms, so that only the depth contributions to RHC presented here would require recalculation.

This work is still in an early stage and a number of technical improvements may be made. Adjustment of the original data for XBT biases should be made before further analysis, as bias-corrected datasets become available. An improved spatial infilling may be possible based on using different space and timescales, or variability functions, for the isotherm depths and mean temperatures, as they represent different dynamic or thermodynamic processes. A more complete vertical description of RHC changes is needed, by combining the analyses for multiple isotherms. The idea is to select a different isotherm at each grid box with a time-mean depth equal to e.g. 300m. This will maximise the observational coverage and allow a more direct comparison with fixed depth OHC analyses. An improved error analysis of the heat content changes should also be possible based on the separation of most of the high frequency, dynamical, noise into the isotherm depth variability.

The important conclusions emerging for ocean climate are that the phase of decadal climate modes leave a strong imprint in local heat content changes, but mainly via a dynamical displacement of isotherms. On the basin and global scale this advective contribution to heat content change is generally small, except in the North Atlantic where there is evidence for a large advective signal over the historical record. This should allow improved quantification of the externally driven surface heat flux induced warming. The separate contributions to heat content variability can be useful for detection and attribution studies with coupled climate models. If the internal dynamical signals in ocean heat content variability, (ranging from internal waves to low frequency climate mode, NAO, PDO and so forth) can be separated, then the externally driven variations from surface flux induced warming, represented by mean temperature above isotherms, should have a higher signal-to-noise

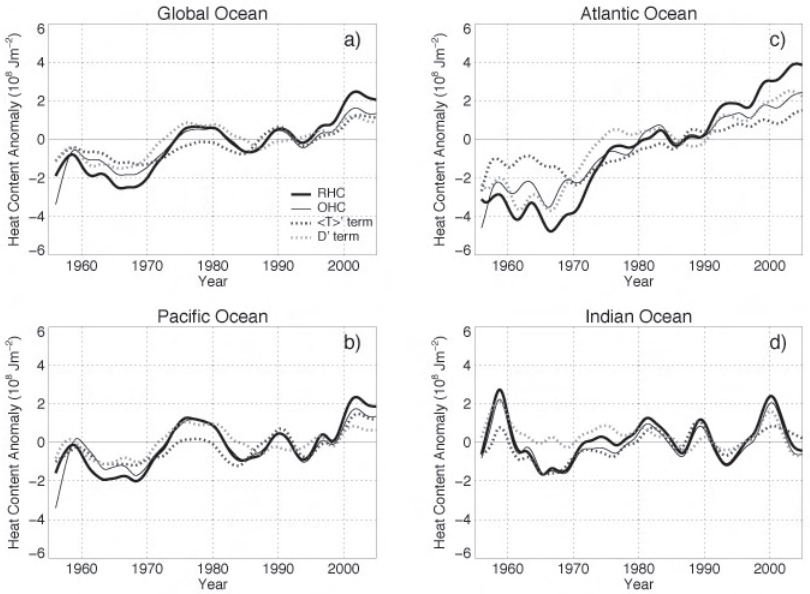

Figure 2: 5-year low-passed time series of relative heat content (RHC) anomaly for the Tref = 14°C isotherm and contributions from temperature (<T>′ term) and depth (D′ term) variations and OHC in the upper 220m for: (a) Global Ocean; (b) Pacific Ocean; (c) Atlantic Ocean; and (d) Indian Ocean.

ratio and be more comparable between climate models and observations. Preliminary studies with the Met Office Hadley Centre HadCM3 and HadGEM1 climate models are underway.

References:

Barnett T.P., D.W. Pierce, K.M. AchutaRao, P.J. Glecker, B.D. Santer, J.M. Gregory and W.M. Washington, 2005: Penetration of human-induced warming into the worlds oceans, *Science*, **309**, 284-287

Bindoff, N.L., J. Willebrand, V. Artale, A, Cazenave, J. Gregory, S. Gulev, K. Hanawa, C. Le Quéré, S. Levitus, Y. Nojiri, C.K. Shum, L.D. Talley and A. Unnikrishnan, 2007: Observations: Oceanic Climate Change and Sea Level. In: *Climate Change 2007: The Physical Science Basis*. Contribution of Working Group I to the Fourth Assessment Report of the Intergovernmental Panel on Climate Change (Solomon, S., D. Qin, M. Manning, Z. Chen, M. Marquis, K.B. Averyt, M. Tignor and H.L. Miller (eds.)). Cambridge University Press, Cambridge, United Kingdom and New York, NY, USA.

Domingues, C.M., J.A. Church, N.J. White, P.J. Gleckler, S.E. Wijffels, P.M. Barker and J.R. Dunn, 2008: Improved estimates of upper-ocean warming and multi-decadal sea-level rise, *Nature*, **453**, 1090-1094.

Harrison, D.E. and M. Carson, 2007: Is the World ocean warming? Upper-ocean temperature trends: 1950-2000, *J. Phys. Oceanogr.*, **37**, 174-187.

Ingleby, B. and M. Huddleston, 2007: Quality control of ocean temperature and salinity profiles – historical and real time data, *J. Mar. Sys.*, **65**, 158-175.

Palmer M.D., K. Haines, S.F.B. Tett and T.J. Ansell, 2007: Isolating the signal of ocean global warming, *Geophys. Res. Lett.*, **34**, L23610, doi:10.1029/2007GL031712.

Palmer M.D., and K. Haines, 2008: Estimating oceanic heat content change using isotherms, *Submitted to J. Climate*.

Parker, D., C. Folland, A. Scaife, J. Knight, A.Colman, P. Baines, and B. Dong, 2007: Decadal to multidecadal variability and the climate change background. *J. Geophys. Res. (Atmospheres)*, **112**, doi: 10.1029/2007JD008411.

Pierce, D.W., T.P. Barnett, K. AchutaRao, P.J. Glecker, J.M. Gregory and W.M. Washington, 2006: Anthropogenic warming of the oceans: Observaitons and model results, *J. Climate*, **19**, 1873-1900.

Visbeck, M., E. Chassignet, R. Curry, T. Delworth, B. Dickson and G. Krahmann, 2003: The Ocean's Response to North Atlantic Oscillation Variability, in The North Atlantic Oscillation: Climatic Significance and Environmental Impact (J.W. Hurrell, Y. Kushnir, G. Ottersen and M. Visbeck (Eds)), *Geophysical Monograph Series*, **134**, 113-146, 2003.

Wijffels, S.E., J. Willis, C.M. Domingues, P. Baker, N.J. White, A. Gronell, K. Ridgway and J.A. Church, 2008: Changing eXpendable Bathythermograph Fall-rates and their Impact on Estimates of Thermosteric Sea Level Rise, *J. Climate., in press*.

The Role of West African Coastal Upwelling in the Genesis of Tropical Cyclones: a New Mechanism

Diaz, M., and F. Semazzi
North Carolina State University, Raleigh NC, 27695, USA
Corresponding author: mldiaz@ncsu.edu

Introduction

It is still unknown as to why some westward moving mesoscale convective disturbances exiting West Africa at approximately 12°N amplify into tropical cyclones, but others do not,. Recently Sall et al. (2005) have reaffirmed that, at the end of their continental path, most mesoscale convective systems (MCS) weaken and vanish over the ocean, while only a few of them strengthen. This seems to be the case even when the departing MCS appears well developed and the large scale environment is favorable for tropical cyclogenesis. Sall et al (2005) have constructed a cyclogenesis index for the development of tropical cyclones from pre-existing MCSs based on several dynamic and thermodynamic parameters, most of which were also adopted earlier by Gray et al. (1999) in their empirical models for the prediction of seasonal Atlantic tropical cyclone activity. However, Sall et al (2005) have deliberately excluded a sea surface temperature (SST) parameter, because they have concluded that, since summer SST in the region where MCSs enter the eastern Atlantic consistently exceeds the 26.5°C threshold required for tropical cyclogenesis, it is not a determining parameter.

In the present study, we investigate a new mechanism related to tropical cyclogenesis associated with upwelling along the northwestern coast of Africa. As one of the most prominent upwelling regions in the world's oceans, these coastal waters are significantly colder than one would expect at such low latitudes. Driven by persistent northeasterly Trade Winds, which blow parallel to the coast, this upwelling produces the southward flowing Canary Current, which entrains the chilled coastal waters and eventually merges into the North Equatorial Current (Mittelstaedt, 1991). The interaction between this upwelling and the large scale ocean currents allows the cold, upwelled water to be advected farther offshore and southward (Mittelstaedt, 1991). This structure of ocean currents produces a frontal zone in the SST field off the coast of Mauritania during summer. We postulate that the variability of SST along the West African coast, associated with upwelling, may have a profound influence on the development of tropical cyclones in the eastern Atlantic.

Hypothesis

We hypothesize that the position of the upwelling front off the Mauritanian coast modulates the intensity of convective systems leaving the west coast of Africa and affects their prospects for becoming tropical cyclones. When the upwelling front is displaced farther southward (northward), a condition which produces anomalously cold (warm) water off the coast of Mauritania, the intensity of MCSs entering the eastern Atlantic and the potential for tropical cyclogenesis will decrease (increase). We believe that these SST anomalies, which lie to the north of the main MCS trajectory, could be of equal importance to those directly underlying the convection, since the SST near the African coast over which most MCSs traverse has little interannual variability. We note from Figure 1 (page 15) that in August the SST off the African coast south of 15°N has a standard deviation of only about 0.35°C, whereas the corresponding standard deviation along the upwelling front is on the order of 1.0°C.

In order to explain how this upwelling can affect convection well to the south, we must first describe several key aspects of the eastern Atlantic climate system. Along with upwelling, the eastern Atlantic ocean basin off the northwest African coast is characterized by strong isentropic descent, which is driven by a combination of the northerly wind at low levels on the eastern side of the subtropical Azores high, and the warm air aloft, which is advected from the Sahara by the African Easterly Jet. This descending air results in a southward flux of dry air along the West African coast into the monsoon trough. Easterly wave disturbances within the monsoon trough strongly enhance this flux along the West African coast, since they produce meridional wind perturbations. Both observational and model analyses (not shown) confirm the southward flux of dry air produced by isentropic descent and reveal a minimum in average specific humidity, collocated with the upwelling region, from about 18°N-24°N at approximately 950–900 mb. This dry air, in combination with cold SST and warm air aloft from the Sahara, produces very strong static stability within the upwelling region. Thus, the airmass off the Mauritanian coast is extremely unfavorable for convection.

We hypothesize that the connection between easterly wave convection, tropical cyclogenesis, and upwelling involves the following sequence of developments: the northerly wind perturbation associated with an easterly wave advects the dry, stable airmass southward. This airmass is moistened and cooled by fluxes from the ocean. When the upwind SSTs are anomalously cold (i.e. stronger upwelling), the southward flowing air, which impacts the convection leaving the African coast, remains drier and more stable. This drier, more stable air tends to weaken easterly wave convection and lower the probability of subsequent development of tropical cyclones. The opposite effect occurs when the SST is anomalously warm.

Empirical Analysis

Figure 1 illustrates our motivation for the proposed mechanism that combines coastal upwelling and convection by comparing NOAA Optimum Interpolation Sea Surface Temperature V2 (Reynolds et al., 2002) and NOAA Interpolated Outgoing Longwave Radiation (Liebmann and Smith, 1996), which is a good proxy for convection. Using data from 1982-2007, correlation coefficients between August average SST and August average OLR in a box bounded by 8°N-15°N and 35°W-15°W are calculated and overlaid with SST standard deviation. This box is centered along the typical track of an easterly wave which exits the African coast. Negative values indicate that warm SST accompanies enhanced convection and vice versa. Based on 26 years of data, correlation coefficients of 0.388 are significant at the 95th percentile and coefficients of 0.495 are significant at the 99th percentile. Note the strong correlation with coefficients numerically in excess of -0.55 between convection off the African coast and the SST in the vicinity of the upwelling front, whose position is revealed by the maximum in standard deviation between 18°N-20°N. In fact, according to this same dataset, this region has the largest SST standard deviation in the entire North Atlantic south of 40°N during August. Based on this evidence, we conclude that convection off the coast of Africa is related to the position of the upwelling front. Nevertheless, it remains unclear whether this signal is the result of a general enhancement of convection or a direct result of tropical cyclogenesis.

To examine how upwelling relates to tropical cyclogenesis in the eastern Atlantic, we use the same SST dataset for August 1982-2007 used previously and compare it with the number of tropical cyclones that formed east of 60°W during July and August. To eliminate the direct effect of underlying SST on tropical cyclogenesis near the upwelling region itself, we eliminate tropical cyclones forming both east of 30°W and north of 15°N from this count. Figure 2 (page 15) shows the correlation coefficients between SST and tropical cyclogenesis overlaid with average August SST. Significance levels are the same as those defined for Figure 1. Again, note the high positive correlations (values > 0.55) along the upwelling front well to the north of where tropical cyclogenesis typically occurs. By September, however, this relationship becomes weaker, though still noticeable, as the upwelling front reaches its northernmost extent. Thus, it appears that this mechanism operates most strongly during July and August. It is important to note that the high correlations between Atlantic hurricanes and SST well to the north have already been found (Shapiro, 1982). They have often been explained by suggesting that years with anomalously weak wind shear, a condition favoring tropical cyclogenesis, tend to be associated with warm SST throughout the tropical north Atlantic. Thus, the warmer SSTs may not directly enhance seasonal tropical cyclone activity to the extent that the high correlations would suggest. Although this relationship may be true, this study attempts to directly link these warmer SSTs along the African coast with tropical cyclogenesis. Additionally, Shapiro and Goldenberg (1997) found a relationship between seasonal hurricane activity in the Atlantic and seasonally averaged SST which is independent of wind shear. In contrast to our investigation, they focused on hurricanes only. The mechanism we have proposed focuses on the transition of tropical disturbances into tropical cyclones.

Numerical modeling

To test our hypothesis, we have performed a series of numerical experiments using the WRF V 3.0 ARW (Weather Research and Forecasting Model) to simulate the genesis and growth of hurricane Ernesto from August 15 to August 23 of 2006. The model domain consists of a coarse domain with 30 km grid spacing, which covers 69°W-9°E and 2.5°S-34°N, and a fine domain of 10 km grid spacing, which follows the incipient tropical cyclone, with dimensions of 14° of latitude and 15° of longitude. We use the Global Forecast System (GFS) as initial and boundary conditions. Although the control simulation produces a 969 mb hurricane before the historical Ernesto even becomes a named storm, the intention is simply to model an easterly wave exiting the coast of Africa and becoming a tropical cyclone, rather than to try to simulate the historical event. For the experiments, we imposed four different SST anomaly patterns, three of them negative and one positive. For the first three experiments, we adopt simple rectangular geometry for the anomaly patterns and the following identification conventions: "box 1" covers the region 15°N-22°N, 16°W-20°W, and "box 2" corresponds to the area 15°N-22°N, 20°W-24°W. For Experiment 1 (Exp. 1) we prescribe a 4°C cold anomaly in box 1 and a 2°C cold anomaly in box 2. Experiment 2 (Exp. 2) is the same as Exp. 1, except that the anomalies are reduced by half. Experiment 3 (Exp. 3) is the same as Exp. 2, except with positive anomalies

contd. on page 17

From Gemmell et al, page 7: Evaluation of water masses in ocean syntheses products

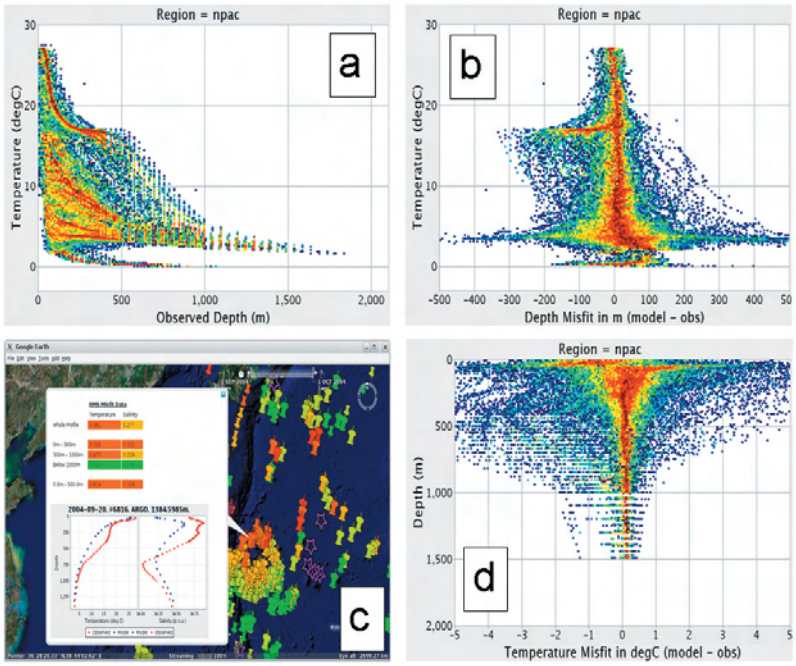

Fig 1 (a) z(T) probability density functions of observed profiles for September 2004 in the North Pacific (b) Misfit in z(T) for these profiles compared to the WOA05 climatology, (c) Typical temperature profiles in the North Pacific Mode Water region from observations and from WOA05, sampled from OceanDIVA's Google Earth display. (d) Misfits in T(z) for the profiles compared to the WOA05 climatology.

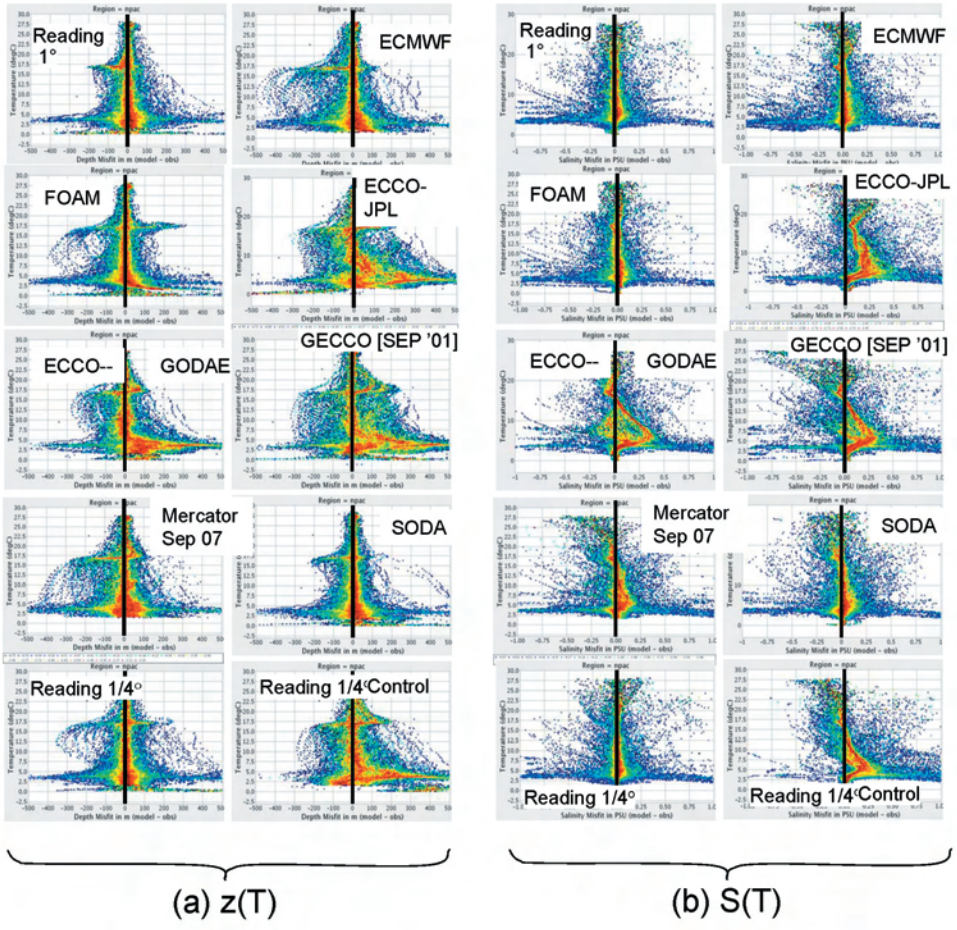

Fig 2 Probability density functions of z(T) misfits in the North Pacific (a), and S(T) misfits in the North Pacific (b), against September 2004 profile data for some of the synthesis products described in Table 1. Saline (fresh) biases in the syntheses are positive (negative). All model data are from September 2004, except GECCO from Sept 01 and Mercator from Sept 07.

From Gemmell et al, page 7: Evaluation of water masses in ocean syntheses products

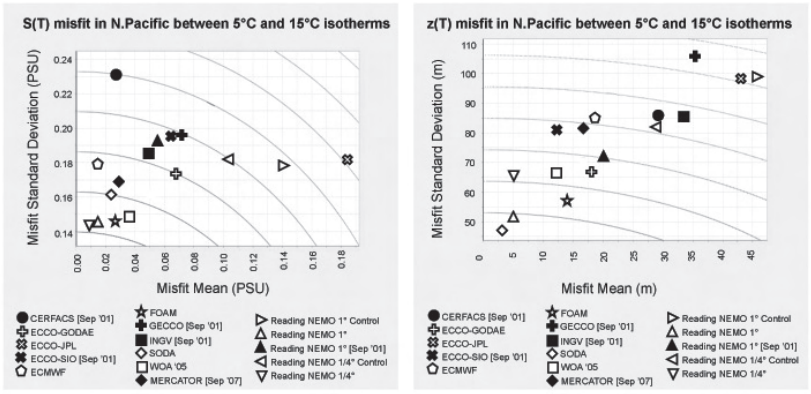

Figure 3 Standard deviation against mean misfit for the syntheses in table 1 for September 2004 in the North Pacific, between the 5°C and 15°C isotherms. The left panel shows S(T) misfit characteristics, whilst the right panel shows z(T) misfit characteristics. Radii of total RMS misfit are also shown (contour levels 0.01psu and 5m respectively).

Figure 4 Standard deviation versus mean misfit for syntheses in table 1 for September 2004 for a) z(T) misfit for the North Pacific subtropical mode water (16-18°C isotherms), and b) Global S(T) misfit for isotherms between 5-15°C . Radii of total RMS misfit are also shown.

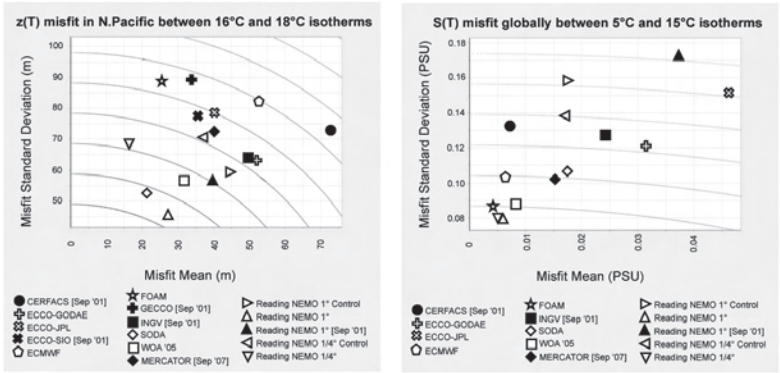

From Haines and Palmer, page 9: On isothermal diagnostics of ocean heat content

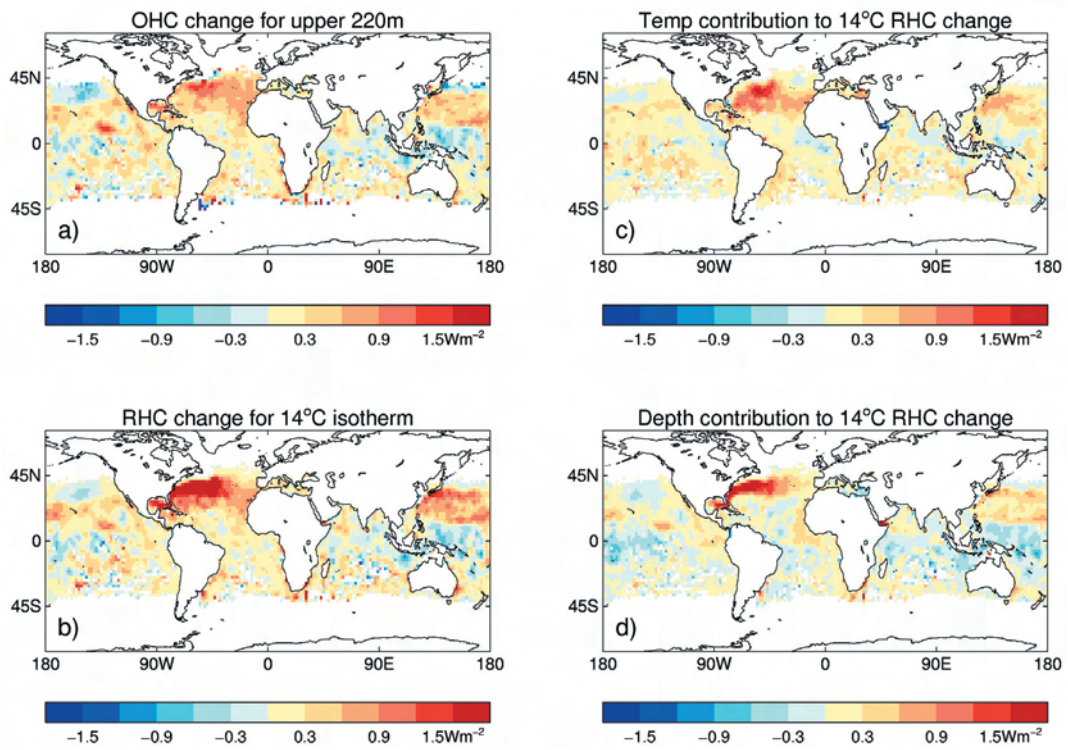

Figure 1: a) 1995-2004 minus 1965-1974 change in OHC for the upper 220m; b) 1995-2004 minus 1965-1974 change in RHC for Tref = 14°C; c) as b, but isolating the temperature contribution to RHC change; d) as b, but isolating the depth contribution to RHC change. Positive features indicate oceanic heat gain for the later period. Changes are expressed as an equivalent time-mean surface heat flux over a 30 year period. A 1:2:1 smoothing has been applied in the north-south and east-west directions.

From Diaz et al., page 11: The Role of West African Coastal Upwelling in the Genesis of Tropical Cyclones: a New Mechanism

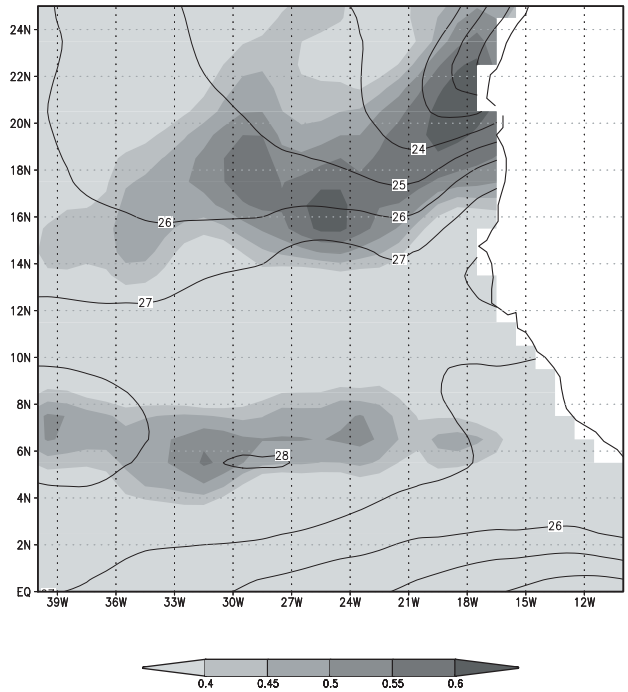

Figure 1. Correlation coefficients between August 1982-2007 OLR and SST (shaded) overlaid with SST standard deviation (°C) .

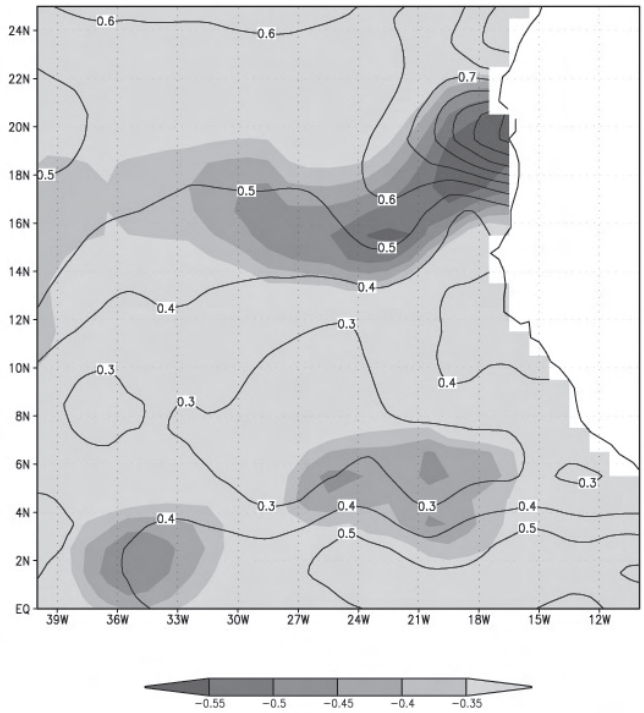

Figure 2. Correlation coefficients between July and August tropical cyclones forming east of 60°W and August SST (°C) from 1982-2007 (shaded). Contour lines show average August SST from 1982-2007.

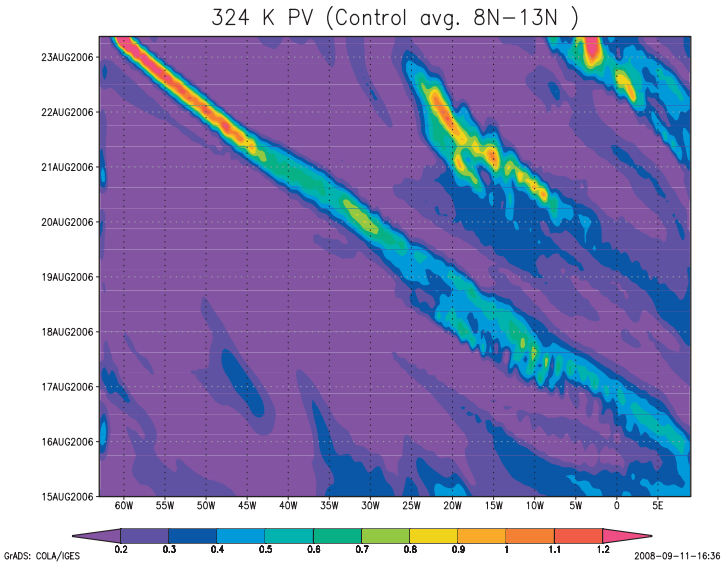

Figure 3. Hovmöller plot of potential vorticity in PVU on the 324 K isentropic surface averaged from 8°N-13°N for the control run.

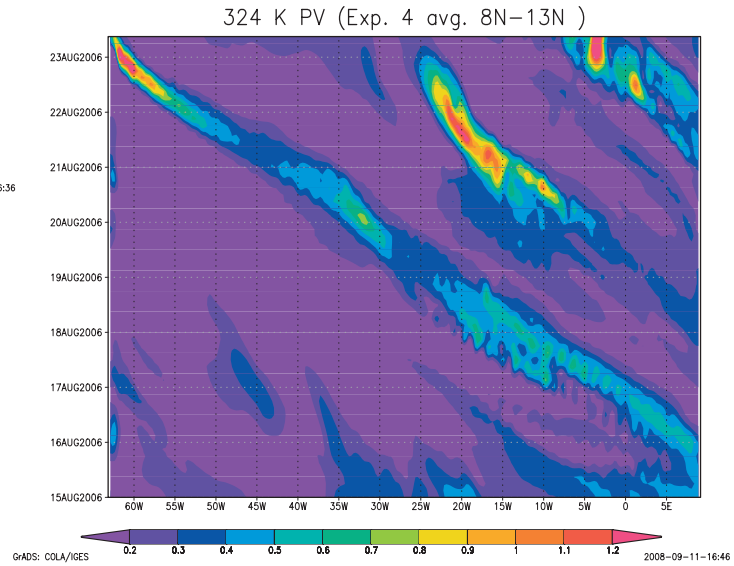

Figure 4. Hovmöller plot of potential vorticity in PVU on the 324 K isentropic surface averaged from 8°N-13°N for Exp. 4.

From Gottschalck et al., page 18: Madden-Julian Oscillation Forecasting at Operational Modelling Centres

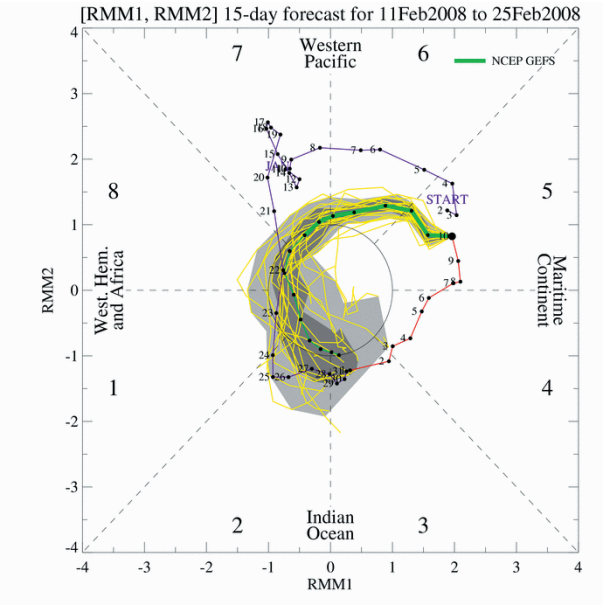

Figure 1: Example 15-day forecasts of the RMM indices from the Global Ensemble Forecast System (GEFS) from the National Centres for Environmental Prediction (NCEP) initialized on the 10 February 2008. The two axes are respectively the first and second projection coefficients of the model output onto the observed empirical orthogonal function structures of the MJO, called RMM1 and RMM2. Anti-clockwise rotation in this phase space represents eastward propagation of the MJO. The GEFS is an ensemble forecast system consisting of 20 ensemble members. The green line is the ensemble mean MJO forecast (week 1 - thick line; week 2 - thin line), the yellow lines are the forecasts from the 20 ensemble members (unperturbed ensemble member) and the red and blue line represents the observational values for the previous 40 days. The light gray shading indicates the spread of 90% of the ensemble members and the dark gray indicates the spread of the middle 50% of ensemble members. Each dot represents a day, extending from the analysis on 2 January to the last day of the forecast on 25 February.

From Maia et al., page 23: Quantifying climate-related risks and uncertainties using Cox regression models.

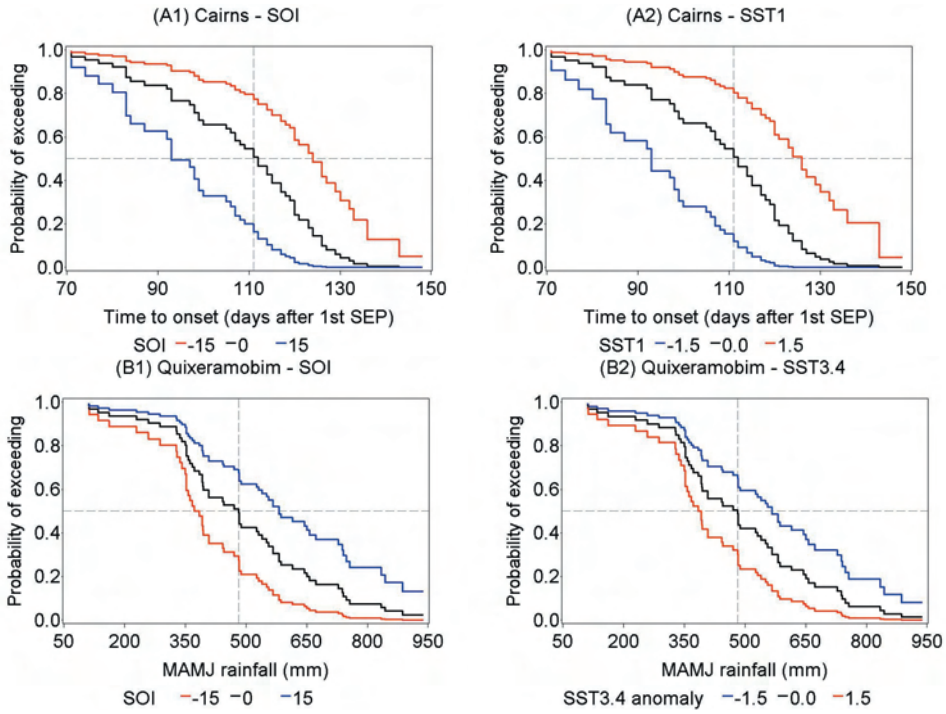

Figure 1: Probability of exceeding functions estimated using CoxPH models. Top panels show forecast time to wet season onset at Cairns based on preceding values of JJA SOI (A1) and JJA SST1 (A2), using empirical rainfall records (1949-2005). Onset was defined as the accumulation of 15% total rainfall wet season rainfall. Bottom panels show seasonal wet season rainfall (MAMJ) for Quixeramobim based on preceding values of Dec – Feb SOI (B1) and Oct - Feb SST3.4 (B2), using empirical rainfall records (1950-2007). The vertical dashed lines indicate median time to onset (Cairns) or median wet season rainfall (Quixeramobim); the solid black lines indicate empirical climatology.

contd. from page 12

instead of negative ones. In Experiment 4 (Exp. 4), instead of simple rectangular geometry, we impose a negative SST anomaly pattern north of 15°N and east of 30°W, which is equal to the difference between the average July 2006 and August 2006 SST. Although each of these anomaly patterns is more extreme than would typically be observed, the larger magnitude of the changes allows their effect to be more easily isolated.

Results

The results of the numerical experiments agree well with our hypothesis. The minimum central pressure (mb) of the disturbance on 06Z Aug. 23 for each of the four simulation is as follows: Control, 969 mb, Exp. 1, 997, Exp. 2, 1009, Exp. 3, 971, Exp. 4, 1009. Thus, both the control and the positive anomaly simulation develop a strong hurricane, with little difference between the two. However, all three of the cold anomaly simulations develop either a weak system or none at all. It is surprising that the strongest storm is not produced in Exp. 3, which contains the warmest anomalies and the weakest in Exp. 1, which contains the coldest anomalies. This outcome suggests that the relationship between SST anomalies and tropical cyclogenesis is nonlinear. Nevertheless, there is still strong agreement among these experiments that the cold anomalies have a negative impact on tropical cyclogenesis in the numerical model results.

To investigate if the influx of dry air inhibits the easterly wave convection and thus suppresses tropical cyclogenesis, we examine difference fields of specific humidity on the 305 K isentropic surface (not shown). This surface passes through the boundary layer within the upwelling region and above it south of the upwelling. The results indicate that a deficit of about 1-4 g/kg in the cold anomaly cases originates from the upwelling region and spirals into the circulation (not shown). Consistent with the cold anomaly experiments, the warm SST anomaly case produces a 1-2 g/kg surplus of moisture relative to the control case which is advected into the tropical disturbance from the upwelling region. Back trajectories through the lower troposphere confirm that the tropical disturbance does contain air parcels which track back to the coast of Africa through the upwelling region (not shown). Comparing total precipitable water in a box around the developing systems also indicates a strong tendency for the cold anomaly cases to be drier than the control case and the warm anomaly case to be moister than the control case (not shown). To summarize the results of these experiments most succinctly, we compare Hovmöller plots of potential vorticity (PV) on the 324 K isentropic surface averaged from 8°N-13°N for the control case and Exp. 4 (Figures 3 and 4 respectively on page 15). The 324 K isentropic surface is located in the middle troposphere and captures the PV maxima associated with deep convection leaving the coast of Africa which remain collocated with their associated easterly wave. In both cases, we clearly note the striking continuity between the African convection and the developing tropical cyclone. However, after leaving the African coast near 17°W, the PV maxima in Exp. 4 (Figure 4) become weaker relative to the control (Figure 3). We attribute this difference to the weakening of the convection due to the entrainment of drier, more stable air from the upwelling coastal region to the north of where the easterly wave enters the eastern Atlantic. The weaker PV maxima in Exp. 4 tend to induce a weaker surface circulation and thus delay or prohibit future tropical cyclogenesis. The other three experiments yield similar interpretations.

Conclusions

Our main finding is that the coastal waters off northwestern Africa north of 15°N may be an important moisture source for tropical cyclones developing in the eastern Atlantic. This source tends to offset the detrimental effects associated with the horizontal flux of extremely dry northeastern Atlantic air. Since the presence of an upwelling front leads to large interannual SST variability in this region, we postulate that the flux of moisture into the monsoon trough along the African coast also experiences large year to year variability. As shown with both our observational and model analyses, a southward displacement of this front favors stronger convection off the African coast and the potential for an increased number of tropical cyclones downwind of this region in the eastern Atlantic Ocean basin. Further investigation of the proposed mechanisms will be the subject of future investigation.

References

Gray, W.M., C.W. Landsea, P.W. Mielke Jr., and K.J. Berry, 1999: Forecast of Atlantic seasonal hurricane activity for 1999. *Dept. of Atmos. Sci. Report*, Colo. State Univ., Ft. Collins, CO, released on 4 June, 1999.

Liebmann, B. and C. A. Smith, 1996: Description of a Complete (Interpolated) Outgoing Longwave Radiation Dataset. *Bulletin of the American Meteorological Society*, **77**, 1275-1277.

Mittelstaedt, E., 1991: The ocean boundary along the northwest African coast: Circulation and oceanographic properties at the sea surface. *Progress in Oceanography*, **26**, 207-355.

Reynolds, R.W., N.A. Rayner, T.M. Smith, D.C. Stokes, and W. Wang, 2002: An improved in situ and satellite SST analysis for climate. *J. Climate*, **15**, 1609-1625.

Sall., A.M., H. Sauvageot, A. T. Gaye, A. Viltard, and P. Felice, 2005: A cyclogenesis index for tropical Atlantic off the African coasts. *Atmospheric Research*, **79**, 123–147.

Shapiro, L. J., 1982: Hurricane climatic fluctuations. Part II: relation to large-scale circulation. *Monthly Weather Review*, **10**, 1014-1023.

Shapiro, L. J., and S. B. Golderberg, 1997: Atlantic sea surface temperatures and tropical cyclone formation. *Journal of Climate*, **11**, 578-590.

CONFERENCE ANNOUNCEMENT

3rd International AMMA Conference will take place from 20th to 24th July 2009 in Ouagadougou, Burkina Faso.

"The 3rd AMMA Conference aims to bring together researchers from around the world working on the West African Monsoon and its impacts, to review ongoing research activities and to discuss future contributions and directions within the AMMA research programme. It also provides an ideal opportunity to broadcast the new knowledge towards the African community."

Madden–Julian Oscillation Forecasting at Operational Modelling Centres

Gottschalck, J.[1], M. Wheeler2, K. Weickmann[3], D. Waliser[4], K. Sperber[5], F. Vitart[6], N. Savage[7], H. Lin[8], H. Hendon[4], M. Flatau[9]
[1]NOAA, USA.; [2]Australian Bureau of Meteorology; [3]NOAA – Earth System Research Laboratory, SA; [4]Jet Propulsion Laboratory, California Institute of Technology, USA.; [5]Lawrence Livermore National Laboratory, USA.; [6]ECMWF, Reading, UK; [7]UK Met Office Exeter. UK; [8]Environment Canada; [9]Naval Research Laboratory, Monterey California, USA.
Corresponding author: Jon.Gottschalck@noaa.gov

1 Background

During late 2007, the U.S. Climate Variability and Predictability (CLIVAR) Madden-Julian Oscillation (MJO) working group[1] (MJOWG) began outlining a strategy to develop and apply a uniform metric for real-time dynamical MJO forecasts. Such a metric, and its utility, would be analogous for example to the pattern correlation of the 500 hPa geopotential heights for weather forecasts or the skill measures in predicting the Niño 3.4 SST index for ENSO forecasts. The goals of the activity are to generate further recognition and expertise regarding the intraseasonal time scale, and to work in particular to develop and/or improve intraseasonal forecasts, with an emphasis on the MJO. Advances in computing have led to numerical forecast models, either coupled ocean-atmosphere models or atmosphere-only models, extending their forecast range to 10 days and beyond, thus allowing for more attention to the intraseasonal time scale and MJO. The virtues of developing and employing such a metric are that it will provide: 1) a means to quantitatively compare MJO forecast skill across the Centres, 2) a quantitative way to measure gains in forecast skill over time by a given Centre or the community as a whole, 3) the means by which to judge proposed forecast model improvements relative to their performance on the MJO and 4) facilitate the development of a multi-model forecast of the MJO. This activity is seen as an important step for improved realization of intraseasonal predictions, particularly in the Tropics but also, indirectly, of the low-frequency extra-tropical weather variability influenced by the MJO.

2 Development and Implementation

To solicit participation from the modelling Centres, an invitation letter from the US CLIVAR MJOWG and the Working Group on Numerical Experimentation (WGNE) was distributed. The letter requested contributions in the way of small subsets of data from Centres' operational medium-range and/or seasonal prediction systems, including their ensembles, for computation of the standard MJO metric. The MJO metric developed for this activity was based on extensive deliberations amongst members of the MJOWG in conjunction with input from a number of Centres. It follows very closely the two-component index (i.e. RMM1 and RMM2) outlined in Wheeler and Hendon (2004; hereafter WH2004) that is summarized in section 3. Since no temporal filtering is required, the indices are extremely useful for real-time applications. In recent years, they have been adopted in a number of applications by the MJO research and forecasting communities, with the latter being mainly focused on statistical methods and applications. More recently, the indices have been applied to forecast data from dynamical forecast model output (Seo *et al*., 2008; Savage and Milton 2007; Lin *et al*., 2008). These studies, however, have used different datasets and methodologies in production of the real-time WH2004 style phase diagrams along with varying levels of, and specifics for, verification statistics. A consolidation of these efforts was a principle goal of the MJOWG activity. The main difference between the MJO index calculation, as agreed upon by the MJOWG and that described in WH2004, is that the former does not remove the low-frequency variability linearly related to an SST index prior to calculating the indices. The purpose of this step is to remove the interannual variability associated with the ENSO cycle and was deemed unnecessary by the MJOWG for this particular application due to the subsequent removal of the most recent 120-day mean.

To participate, Centres are asked to provide minor data contributions from their forecasts that include three latitudinally-averaged, near-equatorial fields of OLR, zonal winds at 200 hPa and zonal winds at 850 hPa at a 2.5° resolution for each model forecast day. The request also calls for the associated model analysis fields and forecast ensemble members if available. Usually, these systems are run daily, but longer integrations from systems run at a reduced frequency (e.g., monthly or seasonal forecasting systems run weekly), are also sought. The solicitation specifies input of the field data itself, rather than the RMM and MJO indices, to allow for standardization of the calculation across all contributing models. Centres are asked to provide these as total fields from which anomalies are created with respect to a climatological seasonal cycle computed from the NCEP/NCAR Reanalysis for the winds, and satellite observations for the OLR. Additionally, some Centres provide anomalies computed with respect to their own lead-dependent hindcast climatologies, which helps to remove model drift and systematic biases from their forecasts. Details of the required data are given in Table 1. As of writing, the MJOWG has obtained the participation of NCEP, ECMWF, UKMO, ABOM, CMC, CPTEC, and JMA.

3 Current Status

Substantial progress has already been made during the last six months (i.e. first half of 2008) as part of this activity. An ftp area at NCEP has been created to receive the model data from all participating Centres listed above. Moreover, the uniform and agreed upon procedure outlined for calculation of the MJO metric is being applied in real time, with initial evaluation/validation being conducted internally by NCEP. Figure 1 (page 16) illustrates an example of the initially agreed upon phase space display of the calculated two-component MJO metric (i.e. RMM1 and RMM2) based on an ensemble forecast from NCEP. Observations for the last 40 days are displayed along with the model forecasts including ensemble information when available. An experimental web page (under construction) has been developed and is hosted by CPC at the following location: http://www.

[1]*See www.usclivar.org/Organization/MJO_WG.html. The MJO working group also receives support from International CLIVAR, www.clivar.org.*

cpc.ncep.noaa.gov/products/precip/CWlink/MJO/clivar_wh.shtml

The website will not only show the model forecasts illustrated in a standard format but also will display background information on the activity, links to the participating centres, detailed documentation of the methodology and verification statistics. Spatial map representations of the model forecasts will also be displayed in addition to the standard phase space plots described earlier. Although only in its infancy, this activity is already seeing some application in an operational setting as part of preparation of the ABOM's weekly Tropical Climate Note and NCEP's weekly MJO update and Global Tropics Benefits/Hazards Assessment. Further standardizing of the forecasts and their illustration along with systematic verification is expected to increase the usefulness and application of these forecasts and lead to more skillful predictions of the MJO.

4 Future Plans

There are two areas the MJOWG plan to develop/enhance in the coming 1-2 years, in conjunction with the participating Centres. These include: 1) the development and subsequent display of a comprehensive and up to date verification database and analysis, 2) the development of a multi-model ensemble.

Standard verification measures are planned for the evaluation of each Centre's MJO index forecast (i.e. RMM1 and RMM2) against observations and for model inter-comparisons. Stratification by phase of the annual cycle and by MJO event amplitude will also be included as sufficient sample sizes are obtained in the coming years. Although an individual Centre may wish to verify their MJO forecasts against RMM values computed from their own analyses, it has been decided initially that for the overall comparison of the forecasts from the different Centres, the verification will be made against a "multi-model analysis", that is, an analysis computed as an average of the analyses of all contributing Centres. The OLR used in the multi-model verification will be the satellite-observed data. Figure 1 illustrates examples of planned initial verification plots that will appear on the website for the participating models. In order to have a verification benchmark, statistical model predictions as described in Maharaj and Wheeler (2005) and Jiang *et al*., (2008) will be included as part of the verification package.

Data Summary Table	
Fields	OLR, u850, and u200 totals (anomaly fields optional). Initial analysis and forecasts of all ensemble members, out to no more than 40 days.
Resolution	2.5° in longitude (0°, 2.5°E. 5.0°E, ...357.5°E). 15°S-15°N averaged. Daily averaged (00-24Z).
Update frequency	Daily, or less for those systems run at a reduced frequency.
Additional data	At beginning of transfer, send analysis data for past 120 days.
Format	ASCII (text).

Table 1: A table summarizing the data specifics requested of the operational centres participating in the US CLIVAR MJO forecast metric activity

At the current time, two approaches will be explored for developing a multi-model ensemble forecast of the MJO. The first is a straightforward, equally-weighted average between the model ensemble-mean forecasts. The second is an average using historical skill-based weights that account for the independent skill (adjustment for co-linearity) of each ensemble mean forecast. The latter approach is more sophisticated and requires a substantial set of model hindcasts in order compute representative skill measures. The benefits of the second approach are that the weights determined vary as a function of seasonal cycle, lead and model type. However, the number of years of hindcasts required to accurately test the MJO forecast skill is still a topic of investigation and debate. Moreover, it may not be possible for some Centres to perform hindcasts due to computational limitations or Centre priorities, so exact details utilizing this approach as part of a multi-model ensemble are currently unclear. However, if a Centre wishes to, and is able, to perform hindcasts to more rigorously evaluate their forecast skill, our goal would be for them to perform the hindcasts over the most recent years enabling direct comparison of skill with those Centres who choose not to perform hindcasts but yet have been running their operational forecast system for some time.

The above issues and follow-on activities were notable areas of discussion by MJOWG members and operational Centre participants during the International Centre for Theoretical Physics (ICTP) workshop on Multi-scale Predictions of the Asian and African Summer Monsoon during 11-15 August 2008 in Trieste, Italy.

References

Jiang, X., D.E. Waliser, M.C. Wheeler, C. Jones, M.-I. Lee, and S.D. Schubert, 2008: Assessing the skill of an all-season statistical forecast model for the Madden-Julian oscillation. *Mon. Wea. Rev.*,**136**, 1940-1956.

Lin, H., G. Brunet, and J. Derome, 2008: Forecast skill of the Madden-Julian Oscillation in two Canadian atmospheric models. *Mon.Wea. Rev., in press*.

Maharaj, E.A., and M.C. Wheeler, 2005: Forecasting an index of the Madden-oscillation. *Int. J. Climatol*., 25, 1611-1618.

Savage, N. and S. Milton, 2007: Evaluating 15 day ensemble forecasts of the Madden Julian Oscillation. *US CLIVAR MJO workshop*, Nov 2007, Irvine, CA USA.

Seo, K-H, W. Wang, J. Gottschalck, Q. Zhang, J-K. Schemm, W. Higgins, and A. Kumar, 2008: Evaluation of MJO forecast skill from several statistical and dynamical forecast models, *J. Climate, accepted*.

Wheeler, M.C., and H.H. Hendon, 2004: An all-season real-time multivariate MJO Index: Development of an index for monitoring and prediction. *Mon. Wea. Rev.*, **132**, 1917-1932.

Numerical Simulations of the Role of Land Surface Conditions on the Climate of Mt. Kilimanjaro Region

Heuser, S., and F.H.M. Semazzi
Department of Marine, Earth, and Atmospheric Sciences, North Carolina State University, Raleigh, NC, USA
Corresponding author: sean.heuser@gmail.com

Introduction

Tropical glaciers are an important indicator of climate change (Houghton *et al*., 2001; Oerlemans, 2001). Perhaps the best recognized tropical glacier is the cap of Mount Kilimanjaro, located along the boarder of Kenya and Tanzania, which has exhibited dramatic recession during the recent decades. Figure 1 (front cover) shows the glacier extent of Mt. Kilimanjaro between 1993 and 2001 and it has been reported that the amount of ice has decreased by 82% compared to its volume in 1910 (Thompson, 2002). Studies of the Kilimanjaro glacier indicate that the temperature of the region has fluctuated only slightly on the annual timescale (Hastenrath, 1991) and the sharp decrease in precipitation is considered to be the main cause of the glacier recession (Kaser *et al*., 2004).

Mt. Kilimanjaro is located approximately 370 km south of the equator and about the same distance west of the Indian Ocean along the Kenya-Tanzanian border (3°04′S, 37°21′E) (Mölg and Hardy, 2004). At 5893m, Kilimanjaro is the highest mountain in Africa, and its climate is dominated by the biannual passage of the Intertropical Convergence Zone (ITCZ) over the region. There are two distinct rainy seasons typically known as the 'long rains' of March through May and the 'short rains' which occur during the months of October through December. These two seasons account for more than 80% of the precipitation (Coutts, 1969; Basalirwa *et al*., 1999). Thermal homogeneity is observed on the mountain with temperature values varying less than 2°C annually (Hardy *et al*., 1998; Mölg and Hardy, 2004).

Regional climate studies have demonstrated that ENSO and SSTs in the Indian Ocean are the dominant sources of climate variability over eastern Africa (Goddard and Graham, 1999; Yu and Rienecker, 1999; Indeje *et al*., 2000; Clark *et al*., 2003). Schreck and Semazzi (2004) isolated another significant pattern of regional climate variability based on 'short rains' seasonal rainfall data. Their analysis is characterized by positive rainfall anomalies over the northeastern sector of eastern Africa (Ethiopia, Somalia, Kenya, and northern Uganda) and opposite conditions over the southwestern region where Mt. Kilimanjaro is located. This signal has strengthened significantly in recent decades (Bowden and Semazzi, 2007). The Intergovernmental Panel on Climate Change AR4 report (Christensen *et al*., 2007) acknowledges the existence of the Indian Ocean dipole mode, however, future scenarios show that precipitation is most likely to increase over the entire east African region between 2080 and 2099. It is this paradigm that implies the scenario of Kilimanjaro's glacier possibly disappearing but reforming in the late 21st century.

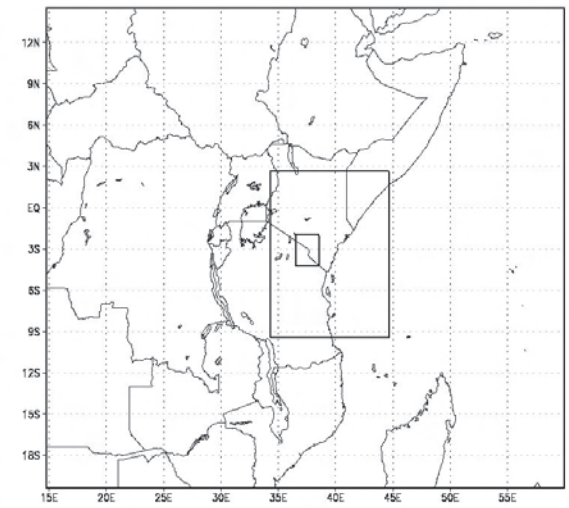

Figure 2: Domains used in Study

Unlike typical mid and high latitude glaciers, which lose their ice during summer with snowmelt and runoff, most of the ice lost on the Kilimanjaro glacier is lost to sublimation (Mölg and Hardy, 2004). Since temperatures vary little annually, changes in the energy balance during the year play a crucial role. The increase in sunlight during the dry season leads to a stronger turbulent latent heat flux, which plays a primary role in the energy balance at the surface (Mölg and Hardy, 2004). This increase in latent heat flux leads to more ice changing phase. However, with temperatures never surpassing the melting point, most of the ice is lost via sublimation.

There are several negative impacts of the receding glacier. For example, one that has generated a lot of concern is the associated increase of forest fires in the deciduous forests south of the peak (Hemp, 2005.) These fires have led to a downward migration of the upper forest line several hundred meters in recent years (Hemp, 2005).

The combination of population increase in the Mt. Kilimanjaro region and decrease in precipitation over the years have resulted in significant changes in vegetation cover and land use. From a meteorological context the change in vegetation affects climate through three primary factors, namely, albedo, surface roughness, and evapotranspiration. We hypothesize that the response of precipitation to land use change is significantly greater than that of temperature, and therefore a more likely factor for modulating the glacial volume over the Mt. Kilimanjaro summit. Initially, in this modeling study, we shall focus on changes in albedo as a proxy for land use change. In future phases of this study we also plan to investigate the role of evapotranspiration & surface roughness.

Design of Model Experiments

We adopt the Advanced Weather Research and Forecast Model (WRF-ARW) model for this investigation. All experiments are based on the year of 2000 which was chosen to minimize the impacts of El Nino and the Indian Ocean Dipole which dominate interannual climate variability. Each experiment is of three months duration from March to May (MAM). A triple-nested grid is used with the coarsest grid resolution of 36km, an intermediate grid of 12 km, and the finest grid of 4km which is centered over Mt. Kilimanjaro. Figure 2 shows the location of each domain used in the study.

The WRF-ARW model is driven by initial, lateral, and

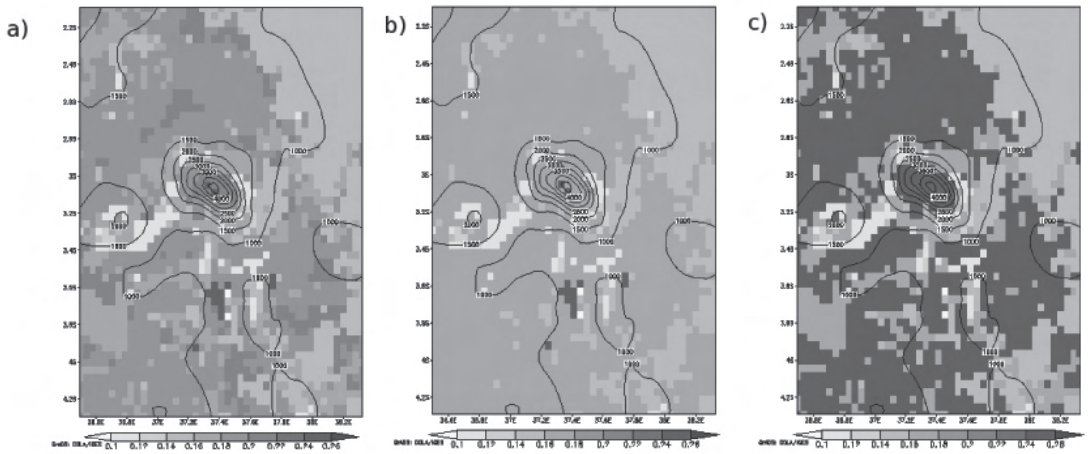

Figure 3: Locations of changed albedo from a) 0.22 simulation(Control), b) 0.18 simulation, and c) 0.25 simulation

lower boundary conditions derived from the NCEP-NCAR Global Forecast Systems' (GFS) Final Reanalysis (fnl). The fnl dataset is a 6-hourly reanalysis at 1° resolution. The version of WRF we use includes several modifications from the standard version of the model. These modifications include a combined linear-exponential functional form for the lateral boundary buffer zone (detailed in Liang *et al*., 2001) and a buffer zone of 10 grid points (compared to the default setting of 5 points) adapted from Giorgi *et al*., (1993). Boundary and surface-layer processes are based on the Monin-Obukhov surface scheme, the Noah land surface model, and the YSU boundary layer scheme. Convective parameterization is based on the Eta Kain-Fritsch scheme (Kain and Fritsch,1993). Microphysical processes are resolved with the WRF Single Moment 3-class microphysics. Radiation schemes are implemented from the NCAR Community Atmospheric Model and include aerosol effects and updated ozone.

Model Simulations

We have conducted three simulations for the MAM season: one with default albedo values, the second where we changed the albedo in the savanna and grassland regions to 0.18, and a final run where we changed the albedo in the same regions to 0.25. Figure 3 shows the albedo distribution for (a) the default albedo of 0.22, (b) the change to 0.18, and (c) the change to 0.25. Furthermore, the points shown have been chosen to be upstream of the flow to examine the effect of circulation changes in regards to the mountain. These sensitivity experiments, based on the most extreme changes in albedo, are designed to give the limiting response that might be expected from the albedo effect. The rational is that if the sensitivity experiments do not yield substantial climate anomalies then the albedo mechanism can be dismissed as a potential factor in explaining the glacier recession that has been observed over the recent decades. In the 0.25 albedo experiment we assume that precipitation in the region from the previous rainy season (the 'short rains' of October-December) is below normal, while in the 0.18 albedo simulation we assume that precipitation from the 'short rains' is above normal.

Results

Temperature: Figures 4a-4b shows 2 meter temperature differences for Domain 3 (4 km resolution grid). The plots indicate that albedo shifts lead to some changes of average temperature ranging from -0.25°C to 0.45°C across the domain; the differences range from -0.15°C to 0°C near the top of the mountain. Temperature differences in areas affected by the change in albedo are strongest with the 0.18 scenario associated with increase in temperatures while the 0.25 scenario results in temperature decrease. Although the changes are negative in both cases near the top of the mountain, area averages indicate that the changes are larger for the 0.25 scenario (0.22°C decrease compared to 0.08°C).

Precipitation: Precipitation difference plots (figures 4c and 4d) show that precipitation is affected markedly by changing albedo. Near the top of Kilimanjaro, precipitation increases in the 0.25 scenario (less vegetation) by 49.87 mm and decreases in the 0.18 scenario (more vegetation) by 122.36 mm. In the 0.18 scenario, the other area of pronounced decrease is on the northwest side (75mm or ~12%). Although precipitation increases are found on the northwest side of the mountain in the 0.25 scenario, surprisingly, significant decreases (82mm or ~20%) also occur, but are shifted to the southeastern side and are more widespread.

Discussion

We note that in both albedo sensitivity experiments, the effect of incoming shortwave radiation plays an important role. In fact, in the 0.25 case, where precipitation increases, a 1.78 W m^{-2} (1.6%) average increase in incoming shortwave radiation is observed at the top of mountain. We hypothesize that this increase in shortwave radiation may drive more intense convection causing further increase in precipitation. Moreover, the increase in shortwave radiation suggests that precipitation in the 0.25 case tends to fall over a shorter period of time with larger amounts of precipitation. However, in the 0.18 scenario, where precipitation decreases, a 0.47 W m^{-2} (0.7%) decrease in incoming shortwave radiation is observed. The decrease in incoming shortwave radiation provides a weaker trigger for convection and may be attributed to more cloud cover for a longer period during this time.

A possible feedback mechanism that could affect glacier mass balance is the increase in latent heat flux over the mountain during this time. Latent heat flux is essential in the sublimation of the glacier. In both scenarios, the increase in latent heat flux not only keeps temperatures lower but also uses more energy to sublimate the glacier atop Kilimanjaro. This sublimation could result in more latent heat being released and could accelerate glacial sublimation over the

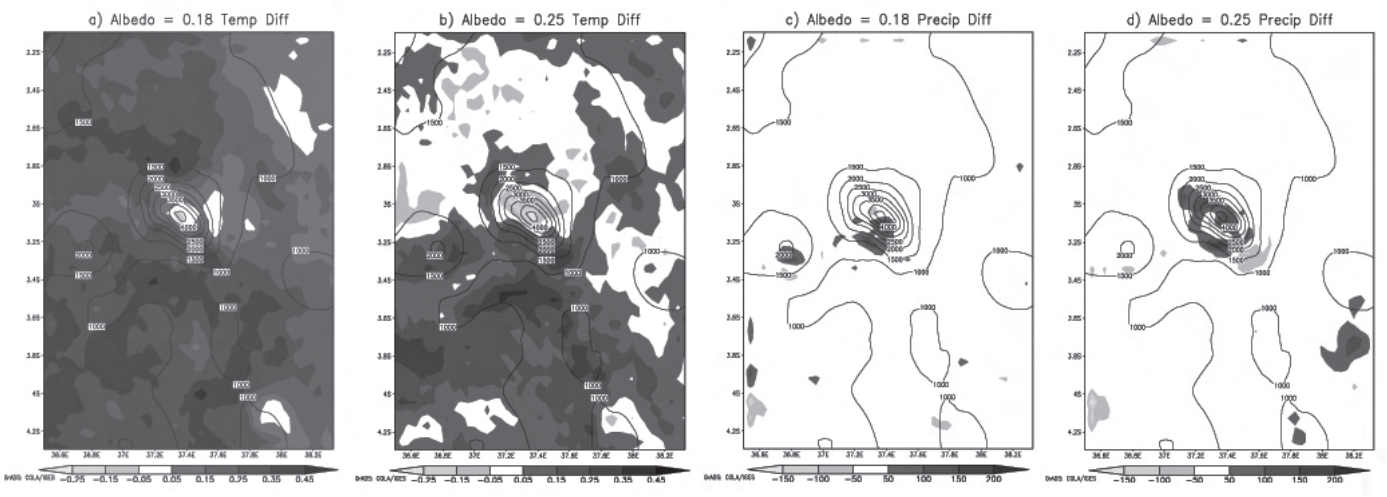

Figure 4: Temperature differences for a) 0.18 simulation – 0.22 simulation, b) 0.25 simulation – 0.22 simulation as well as precipitation differences for c) 0.18 simulation – 0.22 simulation, and d) 0.25 simulation – 0.22 simulation. Temperature values are in degrees C and precipitation values are in mm.

mountain. The increase in precipitation in the 0.25 case would tend to offset this change slightly, but the decrease in precipitation in the 0.18 scenario may be damaging to the mass balance of the glacier.

Precipitation not only plays a role over the summit of the glacier, but also in the region surrounding the mountain. Lake Amboseli, located on the northern side of Kilimanjaro in Kenya is home to many wildlife species. The lake itself is a freshwater lake that gets some of its water from precipitation trickling down the mountain. However, too much precipitation will bring with it volcanic ash and salt salinizing the lake (Dunne and Leopold, 1978). The 0.18 scenario, while having less precipitation over the mountain top, simulates more precipitation on the northern side of the mountain, this could lead to a salinization of Lake Amboseli and the possible loss of less salt-tolerant plants in the region.

Conclusions & Future Work

A series of WRF-ARW model simulations have been carried out to examine the impacts of changing albedo during the short rains of East Africa for the year 2000. Three simulations were performed with a default albedo, an albedo reduction from 0.22 to 0.18, and an albedo increase from 0.22 to 0.25. The changes show small impacts on the seasonal temperature values near the top of the mountain with temperatures decreasing in both cases (0.12% in the 0.25 scenario and 0.02% in the 0.18 scenario). However, precipitation changes are more significant with a 6.6% decrease in the 0.18 case and a 2.5% increase in the 0.25 case. The changes in precipitation are influenced significantly by the amount of shortwave radiation absorbed at the surface. The increase in shortwave radiation in the 0.25 case triggered more convection leading to more precipitation. The opposite effect is noticeable in the 0.18 scenario. These changes led to an increase in latent heat flux which we believe would tend to accelerate sublimation atop the mountain. Our modeling results support our hypothesis that the response of precipitation to land use change is significantly greater than that of temperature, and therefore a more likely factor for modulating the glacial volume over Kilimanjaro summit. Initially we have focused on changes in albedo as a proxy for land use change.

Future work will extend this preliminary investigation to include ensemble simulations, simulations of the seasons of the annual cycle, evapotranspiraton and surface effects of vegetation forcing, and the combined effect of all the three vegetation factors to infer the total effect of vegetation anomalies on glacier recession.

References

Basalirwa, C.P.K., J.O. Odiyo, R.J. Mingodo, E.J. Mpeta, 1999: The climatological regions of Tanzania based on the rainfall characteristics. *International Journal of Climatology* **19**: 69-80.

Bowden, J.H. and F.H.M. Semazzi (2004): Empirical Analysis of Interseasonal Climate Variability over the Greater Horn of Africa. *Journal of Climate* **20**: 5715-5731.

Christensen J.H., B. Hewitson, A. Busuioc, A. Chen, X. Gao, I. Held, R. Jones, R.K. Kolli, W-T. Kwon, R. Laprise, V. Magaña Rueda, L. Mearns, C.G. Menéndez, J. Räisänen, A. Rinke, A. Sarr and P. Whetton, 2007: Regional Climate Projections. In: *Climate Change 2007*: The Physical Science Basis. Contribution of Working Group I to the Fourth Assessment Report of the Intergovernmental Panel on Climate Change [Solomon, S., D. Qin, M. Manning, Z. Chen, M. Marquis, K.B. Averyt, M. Tignor and H.L. Miller (eds.)]. Cambridge University Press, Cambridge, United Kingdom and New York, NY, USA.

Clark, C.O., P.J. Webster, and J.E. Cole, 2003: Interdecadal variability of the relationship between the Indian Ocean zonal mode and east African coastal rainfall anomalies. *J. Clim.*, **16**: 548–554.

Coutt,s H.H., 1969: Rainfall of the Kilimanjaro area. *Weather* **24**: 66-69

Dunne, T. and L.B. Leopard, 1978: Water and Environmental Planning. WH Freeman and Company: San Francisco

Giorgi, F., M. Marinucci, G. Bates, 1993: Development of a second-generation Regional Climate Model (RegCM2). Part II: Convective processes and assimilation of lateral boundary conditions. *J. Climate* **121**: 2814-2832.

Goddard, L. and N.E. Graham, 1999: Importance of the Indian Ocean for simulating rainfall anomalies over eastern and southern Africa. *J. Geophysical Research* **104**: 19099-19116.

Hardy, D.R., M. Vuille, C. Braun, F. Keimig, R.S. Bradley, 1998: Annual and daily meteorological cycles at high altitude on a tropical mountain. *Bulletin of the American Meteorological Society* **79**: 1899-1913

Hastenrath, S. 1991. Climate Dynamics of the Tropics. Kluwer: Dordrecht.

Houghton, J.T., Y. Ding, D.J. Griggs, M. Noguer, P.J. van der hinden, X. Dai, K. Maskell, C.A. Johnson (eds.), 2001: *Climate Change 2001: The Scientific Basis*. Cambridge University Press: Cambridge.

Hemp, A. 2005. Climate change-driven forest fires marginalize the impact of ice cap wasting on Kilimanjaro. *Global Change Biology* **11**:1013-1023.

Indeje, M., F.H.M. Semazzi, and L.J. Ogallo, 2000: ENSO signals in East African rainfall seasons. *Int. J. Climatol*. **20**: 19-46.

Kain, J., and J. Fritsch, 1993: Convective parameterization for mesoscale models: The kain-fritsch scheme. *Meteorological Monographs* **24**: 165-170

Kaser, G., 2004: Modern Glacier Retreat on Kilimanjaro as Evidence of Climate Change: Observations and Facts. *Int. J. Climatol*. **24** : 329-339

Liang, X-Z., K. Kunkel, and A. Samel. Development of a Regional Climate Model for U.S. Midwest Applications. Part I: Sensitivity to Buffer Zone Treatment. *Journal of Climate*. **14**: 4363-4378.

Molg, T., D.R. Hardy, 2004: Ablation and associated energy balance of a horizontal glacier surface on Kilimanjaro. *Journal of Geophysical Research*. **109**

Oerlemans, J., 2001: *Glaciers and Climate Change*. Balkema: Rotterdam.

Schreck, C.J. III and F.H.M. Semazzi, 2004: Variability of the recent climate of Eastern Africa. *Int. J. Climatol*. **24**: 681-701.

Thompson, L.G., Mosley-Thompson. E., Davis, M.E., Henderson, K.A., Brecher, H.H., Zagorodnov, V.S., Mashiotta, T.A., Lin, P-N., Mikhalenko, V.N., Hardy, D.R., Beer, J. 2002. Kilimanjaro Ice Core Records: Evidence of HoloceneClimate Change in Tropical Africa. *Science*. **298**: 589

Yu, L.S. and M.M. Rienecker. 1999. Mechanisms for the Indian Ocean warming during the 1997-1998 El Nino. *Geophysical Research Letters*. **26**: 735-738.

Quantifying climate–related risks and uncertainties using Cox regression models

Maia, A.H.M.[1] and H. Meinke[2]
[1]Embrapa Meio Ambiente, Jaguariúna, SP, Brazil; [2] Centre for Crop Systems Analysis, Plant Sciences Group, Wageningen University, PO Box 430, NL 6700 AK Wageningen, The Netherlands; holger.meinke@wur.nl
Corresponding author: ahmaia@cnpma.embrapa.br

Abstract
For applied climate risk management the probability distributions of decision variables such as rainfall, likely dates of climatic events (e.g. frost, onset of the wet season), crop yields or economic returns can be expressed as cumulative distribution functions (CDFs) or probability exceeding functions (PEFs). Such functions are usually derived from empirical or modelled time-series. For forecast purposes in regions impacted by e.g. the El-Nino Southern Oscillation (ENSO), such functions can be categorised by oceanic or atmospheric indexes (e.g. sea surface temperature anomalies, southern oscillation index). These then allow objective climate impact assessments. Although intuition suggests that the degree of uncertainty associated with CDF estimation could impact decision making, quantitative information regarding the uncertainties surrounding these CDFs is rarely provided. Here we propose Cox-type regression models (CRMs) as a powerful statistical framework for making inferences on CDFs in the context of seasonal climate risk assessments. CRMs are semi-parametric approaches especially tailored for modelling CDFs and associated risk measures (relative risks, hazard ratios) and are usually applied to time-to-event data in other domains (e.g. medicine, engineering, social and political sciences). Beyond providing a powerful means to estimate CDFs from empirical data, the Cox approach allows for ranking and selecting multiple potential predictors and quantifying uncertainties surrounding CDF estimates. Well-established and theoretically sound methods for assessing skill and accuracy of Cox-type forecast systems are also available. To demonstrate the power of the Cox approach, we present two examples: (i) estimation of the onset date of the wet season (Cairns, Australia) and (ii) prediction of total wet season rainfall based on historical records (Quixeramobim, Brazil). This study emphasises the methodological aspects of CRMs and does not discuss the merits or otherwise of the ENSO-based predictors. We conclude that CRMs could play an important role in making GCM output more relevant for decision makers through the provision of application-oriented downscaling techniques.

Introduction
Managers of climate-sensitive industries can incorporate probabilistic forecasts of alternative management options as long as the associated uncertainties are clearly spelled out (Nelson et al., 2007). This is particularly true for agriculture and related sectors where proactive adaptation to climate risk is becoming increasingly important (Meinke and Stone, 2005; Howden et al., 2007). Operational climate risk management requires knowledge about the likely consequences of the future state of the climate systems. Often variables of interest (Y), such as time of onset of the wet season (Lo et al., 2007), rainfall, crop yields (Meinke et al., 1996) or return on investment (Twomlow et al., 2008) are provided as CDFs [P(Y≤y)] or PEFs [P(Y>y)]. Such probabilistic representation of decision variables helps risk managers to conduct rapid assessments of management options. CDFs/PEFs are particularly convenient to summarise time series that are not or only weakly auto-correlated. However, if time series are moderately to strongly auto-correlated, a CDF/PEF summary will result in the loss of some information. The decision variables in our study (likely time to wet season onset and seasonal rainfall amounts) are at most weakly auto-correlated, thus allowing the CDF/PEF representation to convey seasonal climate information (Maia et al., 2007).

Here we propose the use of Cox-type regression models (CRMs), a statistical approach that includes the Cox regression model (Cox, 1972) and its generalizations. By using theoretically sound likelihood-based methods, CRM allows for estimating CDFs and their uncertainties, ranking and selecting multiple risk factors and quantifying their impacts on probabilistic outputs of seasonal forecast systems. CRMs are semi-parametric approaches especially tailored for modelling CDFs and associated risk measures (relative risks, hazard ratios) arising from time-to-event data in other domains (e.g. medicine, engineering, social and political sciences; Allison, 1985).

Our main objectives are to (i) introduce the Cox approach to climate scientists; (ii) demonstrate the power of CRMs for statistical climate forecasting and suggest its use for downscaling GCM output, (iii) provide methods for quantifying the degree of uncertainty of probabilistic forecasts and (iv) extend the use CRMs by replacing time-to-event variables with other quantities of interest (e.g. rainfall). Using examples from two locations (Cairns, Australia and Quixeramobim, Brazil), we outline in detail the use of these techniques, including their potential pitfalls.

Background

CDFs are commonly used to summarize information from studies in biomedical, social and engineering research where the objective is to model the time until the occurrence of a certain event such as death, equipment/component failure, divorce or unemployment. The statistical approaches for making inferences about CDFs are referred to as survival analysis, reliability analysis or event history analysis in the fields of medicine (Collett, 1994), engineering (Crowder et al., 1991) and social sciences (Yamaguchi, 1991), respectively. Survival analysis comprises many tools, including parametric, semi-parametric and non-parametric methods for estimating and comparing CDFs (Lawless, 1982). Survival analysis also allows for the inclusion of incomplete information, referred to as censored data[1] . For instance, when studying wet season onset, censored data can occur, when in dry years the criteria for 'onset' is not reached until the end of the defined wet season period (Lo et al., 2007).

Recently, some authors have proposed the use of survival analysis as an innovative tool for modelling time-to-event variables in natural sciences: Anthony et al. (2007) used a CRM to assess the risk of coral mortality in response to temperature, light and sediment regime, while Gienapp et al. (2005) discuss the utility of survival approaches for predicting phenology under climate change scenarios. In spite of its traditional use and recent extensions to other domains, survival analysis has rarely been used for seasonal climate risk assessments (e.g. Maia and Meinke, 1999; Maia et al., 2007). Here we focus on Cox regression models (Cox, 1972) as a methodological framework for empirical-statistical seasonal forecasts of climate-related variables. However, the approach could equally be applied to CDFs generated by other means, such as coupled ocean-atmosphere models.

The original Cox model assumes proportional hazards (PH), a property related to the absence of interaction between predictor and predictant. This constitutes the simplest Cox-type model and will hereafter be referred to as CoxPH model. In the absence of an appropriate time-dependent covariate, Cox models simply assume an average effect over the range of observed data (Allison, 1995). However, a great variety of generalizations for the CoxPH model are available, allowing for adequate modelling of non-proportional hazards, if necessary.

In summary, the main advantages of using the Cox approaches in climate risk assessments include:

- CRMs do not require assumptions regarding the type of underlying probability distributions of the climate-related variable being modelled (in contrast to, for instance, ordinary least squares multiple linear regression, logistic regression or parametric survival analysis);
- the validity of proportional hazards assumption can be tested and, if needed, CoxPH models can be generalised to more flexible Cox-type non-proportional hazard models;
- estimates of probabilities of exceeding [P(Y>y)] can be simultaneously obtained for multiple thresholds (y), an advantage compared to the alternative approach based on, for instance, logistic regression (Lo et al., 2007) where PEFs were composed by individual estimates of [P(Y>y)] arising from logistic functions, estimated one at a time.
- the influence of many potential predictors on climate risks can be investigated simultaneously - the contribution of each potential predictor can be objectively evaluated via likelihood tests;
- methods for assessing model skill and predictive accuracy are readily available.

For demonstration purposes we use CRMs to estimate time to wet season onset in Northern Australia, based on the state of two ENSO-based predictors prior to the commencement of the wet season. We then extend the method beyond its usual application to time-to-event data by assessing the probabilities of exceeding threshold values of rainfall amounts for the wet season in North-eastern Brazil based on similar predictors.

Further, we provide associated uncertainties for estimated CDFs (predictive accuracy) that might guide decision makers in their choice between alternative decisions that could be based on this information. To our knowledge, this study is the first using CRMs to analyse the linkage among oceanic/atmospheric indexes and climate risks thereby extending the methods to the domain of seasonal climate risk assessments.

Data and Methods

To demonstrate the utility of the approach, we present two examples where we investigate the influence of predictors based on oceanic/atmospheric phenomena such as the Southern Oscillation and warming/cooling of surface water in the Pacific basin (El Niño/La Niña) on rainfall-related variables:

Example I. For Cairns (Northern Australia, 16.93°S, 145.78°E) we quantify the influence of the Southern oscillation Index (SOI) (mean of June to August monthly SOI, JJA SOI) and the first rotated principal component (SST1) of large scale SST anomalies (JJA SST1) on time to onset of the wet season (Drosdowsky and Chambers, 2001). We adopted one of the criteria presented by Lo et al. (2007) for defining wet season onset: the date at which 15% of the long term mean of total summer rainfall (September to April) is first reached (after 1 September and before 31 March). We used a high quality, daily rainfall data set (Haylock and Nicholls, 2000) to calculate the time to wet season onset for each year (1948 to 2004). The monthly SOI series is available at

www.bom.gov.au/climate/current/soihtm1.shtml.

Example II. For Quixeramobim (Northeastern Brazil, 5.08°S, 38.06°W) we quantify the influence of SST anomalies (average Oct - Feb) in the Niño 3.4 region (SST3.4, 5°N to 5°S; 170-120° W) and SOI (average Dec- Feb) on the wet season

[1] *In the context of survival analysis, 'censored data' means that some units of observation have incomplete information regarding time-to-event.*

(MAMJ) rainfall amount (1950 to 2007, from Funceme, Ceará's state meteorological agency; www.funceme.br). SST anomaly data for the same period, are available at www.cpc.noaa.gov/data/indices/sstoi.indices.

For both cases, PEFs and associated uncertainties were estimated via CoxPH models, where the probability of T exceeding a particular value t, given a predictor value of x is given by

$$PEF(t, x) = [PEF_0(t)]^{\exp(x.\beta)}$$

where t is the time to event, $PEF_0(t)$ is the baseline survival function, and β is the unknown model parameter that quantifies the influence of the predictor on the $P(T>t)$. The derivative of $PEF(t,x)$ with respect to t is the so called hazard function $h(t, x)$ that represents the instantaneous failure rate at each time t, for $X=x$. Under the proportional hazards assumption, the hazard ratio $[h(t, x_i)/ h(t, x_j)]$ is supposed to be constant over time for any pair (x_i, x_j) of predictor values.

Here we adopt a terminology more adequate for climate studies, using $PEF(t, x)$ instead the classical notation $S(t, x)$. Further, by replacing the time variable $T=t$ with any other quantity $Y=y$ (as in the case of Quixeramobim, where rainfall is the predictant) we can use CRMs for modelling PEFs for important climate dependent variables such as water stress, crop yields or even economic measures (e.g. farm income). For such variables, the hazard function $h(t,x)$ cannot be interpreted as an instantaneous failure rate, but the methods for estimating PEFs and associated uncertainties remain valid. Confidence bands for PEFs were calculated following methods described in Allison (1995). Here we only present a model for a single predictor, although the model can easily be generalized for multiple predictors.

Results and Discussion

Table 1 shows parameter estimates and respective likelihood tests for CoxPH models used to quantify the average (over time) influence of: (a) June - August average SOI or SST1 on time to onset of the wet season at Cairns (models A1 and A2, respectively) and (b) December – February SOI or October – February SST3.4 anomalies on the seasonal rainfall (MAMJ) at Quixeramobim (model B1 and B2, respectively).

Table 1: Parameter estimates and respective standard errors (SE) for CoxPH models fitted for quantifying the influence of atmospheric/ oceanic predictors on the PEFs for time to onset of the wet season at Cairns, Northern Australia (models A1 and A2) and wet season rainfall amount at Quixeramobim, North-eastern Brazil (models B1 and B2).

Model	Predictor	*b*	*SE*	*exp(b)*	*p**
A1	SOI	0.065	0.017	1.067	0.0002
A2	SST1	-0.757	0.199	0.469	0.0001
B1	SOI	-0.028	0.014	0.972	0.0421
B2	SST3.4	0.862	0.143	3.920	0.0478

** Nominal significance levels arising from the maximum likelihood chi-square tests for the hypotheses $\beta = 0$ (no predictor influence). Estimates for β and the hazard ratio (HR) are denoted by b and exp(b), respectively.*

In Figure 1 (page 16) we show PEF estimates derived from fitted CoxPH models for some specific SOI (-15, 0, and +15) and SST anomaly values (-1.5, 0 and 1.5) at both locations. PEFs could also be easily obtained for any other predictor value.

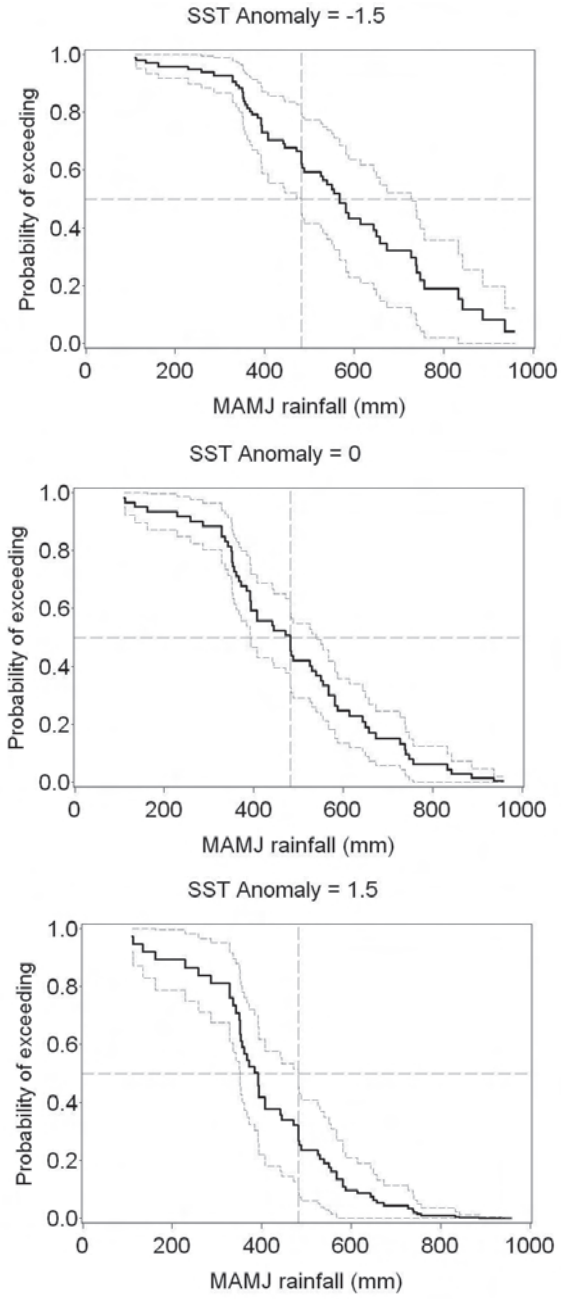

Figure 2: Probability of exceeding functions for MAMJ rainfall at Quixeramobim (Brazil) with respective 95% confidence limits for preceding (October – February) SST3.4 values, estimated via CPH models (as Figure 1B1 and 1B2, page 16).

Using the hazard ratio (HR) estimates from Table 1, we objectively quantify the influence of predictors on PEFs for the climate-related variables. When the HR estimate is grater than one (positive b), for each unitary increase in the predictor, the baseline PEF, $PEF_0(y)$ is powered by the corresponding hazard ratio. As $PEF_0(t)$ has a value between 0 and 1, this results in a decrease in $Prob(Y>y)$.

This occurs for model A1 (Cairns, SOI), for which increases in SOI lead to lower probabilities of late onset and model B2 (Quixeramobim, SST), where increases in SST3.4 lead to lower probabilities of rainfall exceeding a threshold y,

respectively. Conversely, if HR is lower than one (models A2 and B1), unitary increases in predictors lead to increases in *Prob(Y>y)*. These results are consistent with the well known influences of ENSO on the North Australia, where La Niña conditions (positive SOI, negative SST1) favour an earlier than normal start of the wet season (Lo et al., 2007) and on North-eastern Brazil, where El Niño conditions (negative SOI, positive SST3.4 anomalies) lead to low probabilities of substantial wet season rainfall (Coelho et al., 2002).

So far, the PEFs in Figure 1 do not contain any uncertainty estimates. In a final step we expand the risk analysis arising from Model B2 (Quixeramobim, predictor -SSTs.4) by providing their respective 95% asymptotic confidence bands (Figure 2). The width of the confidence limits depends on the series length, the signal strength of the predictor SST3.4 and the predictor value at which the PEF was evaluated.

Given that the main objective of this paper is to show the power of the Cox approach for the generation of seasonal forecasts, we used its simplest form, which assumes proportionality of hazards. Such model might be not able to adequately reproduce some patterns of ENSO influence. In a subsequent step we will refine the risk modelling process by using more flexible non-proportional hazard (NPH) models able to capture nonlinear and possible disproportional influences of ENSO on rainfall-related variables. The use of such models for climate risk assessment as well as a complete evaluation of their skill and predictive accuracy forms part of our ongoing research.

Concluding remarks

In this paper we demonstrate the power of survival analysis, a statistical approach commonly for risk modelling in domains such as medicine, engineering and social sciences. So far these techniques have been undervalued in the domain of climate science, a situation that is likely to continue given the strong focus on dynamical modelling without due attention to the provision of probabilistic forecasts of decision variables such as crop or pasture yields, income or environmental indices, to name just a few. However, particularly for the emerging field of adaptation science, simple, yet locally relevant evaluation techniques are needed. The current trend towards ever increasing complexity in GCM-based modelling without an equal attention to the information needs of decision makers is unlikely to produce such decision-relevant outcomes (Pielke and Sarewitz, 2002).

It has been suggested that using GCMs to predict the driving forces of climate variability might be more robust than carrying the prediction through to highly complex variables such as rainfall (Stone et al., 2000). Given the additional benefit that can be derived from such simple, statistical procedures, we suggest to combine the approaches suggested here with GCM-derived estimates of predictors such as SSTs or SOI to be used as input into statistical models. Such 'downscaling' techniques would enable the provision of information at spatial and temporal scales relevant for decision makers – usually at station to regional scale with a time horizon of up to several years. For practitioners, these are the spatial and temporal scales that really matter and where decisions are made. The statistical techniques presented here also intrinsically account for trends in empirical data. This means that non-stationarity in, for instance, SSTs or SOI values that might be a consequence of climate change are captured by the model. This feature makes it even more attractive to investigate the feasibility of developing a rigorous GCM-CRM interface for provision of user-relevant forecasts risks.

Acknowledgements

HM initiated this work while employed by the Queensland Department of Primary Industries, Australia. The research was financially supported by Land and Water Australia (Managing Climate Variability Program, Project QPI62 - Improving Prediction of the Northern Australian Wet Season). We thank Francis Zwiers for valuable comments on an earlier draft.

References

Allison, P.D., 1995: Survival Analysis Using the SAS® System: A Practical Guide. SAS Institute Inc., 292 pp.

Anthony, K.R.N., S.R. Connolly, O. Hoegh-Guldberg, 2007: Bleaching, energetics, and coral mortality risk: Effects of temperature, light, and sediment regime. *Limnol. Oceanogr*., **52**, 716-726.

Coelho, C.A.S., C.B. Uvo, and T. Ambrizzi, 2002: Exploring the impacts of the tropical Pacific SST on precipitation patterns over South America during ENSO periods. *Theoret. Appl. Climatol*., **1**, 185-197.

Collett, D., 1994: Modelling Survival Data in Medical Research. Chapman and Hall.

Cox, D.R., 1972: Regression models and life-tables (with discussion). *J. Royal Stat. Soc*., **34B**, 187-220.

Crowder, M.J., A.C.Kimber, R.L. Smith, and J. Sweeting, 1991: Statistical Analysis of Reliability Data. Chapman and Hall.

Drosdowsky, W. and L. E. Chambers, 2001: Near-global sea surface temperature anomalies as predictors of Australian seasonal rainfall. *J. Climate*, **14**, 1677-1687.

Gienapp, P., L. Hemerik, and M.E. Visser, 2005: A new statistical tool to predict phenology under climate change scenarios. *Global Change Biol*. **11**, 600-606.

Haylock, M., and N. Nicholls, 2000: Trends in extreme rainfall indices for an updated high quality data set for Australia, 1910-1998. *Int. J. Climatol*., **20**, 1533-1541.

Howden, S.M., J. F. Soussana, F.N. Tubiello, N. Chetri, M. Dunlop, and H. Meinke, 2007: Adapting agriculture to climate change. *Proc. Natl. Acad. Sci*., **104**, 19691-19696.

Lawless, J.E., 1982: Statistical Models and Methods for Lifetime Data, John Wiley & Sons.

Lo, F., M. Wheeler, H. Meinke, and A. Donald, 2007: Probabilistic forecasts of the onset of the north Australian wet season. *Month. Weather Rev*., **135**, 3506-3520.

Maia, A. de H.N., and H. Meinke, 1999: Non-parametrical survival analysis as a statistical tool in agricultural decision making. International Symposium, Modeling Cropping Systems, Proc. Eur. Soc. for Agron. Div. Agroclimatology and Agronomic Modeling, Lleida, Spain, 21-23 June 1999, 103-104.

Maia, A. H. N., H. Meinke, S. Lennox, and R. C. Stone, 2007: Inferential, non-parametric statistics to assess quality of probabilistic forecast systems. *Month. Weather Rev*., **135**, 351-362.

Meinke, H., and R. C. Stone, 2005: Seasonal and inter-annual climate forecasting: The new tool for increasing preparedness to climate variability and change in agricultural planning and operations. Clim. Change, 70, 221-253.

Meinke, H., Stone, R.C. and Hammer, G.L., 1996. Using SOI phases to forecast climatic risk to peanut production: a case study for northern Australia. *Int. J. Climatology*, **16**, 783-789.

Nelson, R., P.Kokic, and H. Meinke, 2007: From rainfall to farm

incomes - transforming policy advice for managing climate risk in Australia. Part II: Forecasting farm incomes. *Aust. J. Agric. Res*., **58**, 1004-1012.

Pielke, R. (Jr); D. Sarewitz, 2002: Wanted: Scientific Leadership on Climate. *Issues in Science and Technology*, **19**: 27.

Stone, R. C., I. Smith, and P. McIntosh, 2000: Statistical methods for deriving seasonal climate forecasts from GCM's. In: Applications of Seasonal Climate Forecasting in Agricultural and Natural Ecosystems, G. L. Hammer, N. Nichols, and C.Mitchell, Eds., Kluwer Academic, 135–147.

Twomlow, S., F. T. Mugabe, M. Mwale, R. Delve, D. Nanja, P.Carberry and M. Howden, 2008: Building adaptive capacity to cope with increasing vulnerability due to climatic change in Africa – a new approach. *Physics and Chemistry of the Earth*, **33**, 780–787.

Yamaguchi, K., 1991: Event history analysis. *Appl. Soc. Res. Meth*., **28**. Sage Publications.

Report on the CLIVAR Pacific Panel Summer School on "ENSO: dynamics and predictability" in Puna, on the Big Island of Hawai'i.

Timmerman, A. and S. Power
on behalf of the organising committee
Corresponding author: axel@hawaii.edu

Fundamental advances have been made in understanding the basic dynamics and predictability of the El Niño-Southern Oscillation (ENSO) phenomenon in recent decades. The breakthroughs strongly depended on (i) the availability of improved observational data sets including the TAO-Triton array, satellite altimeter and SST data, ARGO floats and drifters, wind-stress products, and numerous other atmospheric data sets), (ii) the use of a hierarchy of models from simple analog models, through intermediate coupled models, to coupled general circulation models, and (iii) the insights of researchers over past decades.

While fundamental advances in our understanding have been made, many important questions still remain unanswered. For example:

1. Is ENSO a stable, stochastically, excited mode, or a deterministic unstable oscillation whose amplitude is damped by nonlinearities?
2. What determines the amplitude and skewness of ENSO?
3. Why does ENSO vary on decadal timescales?
4. What is the role of westerly wind-bursts (WWBs) in triggering/driving ENSO variability?
5. How does ENSO interact with the annual cycle
6. How does ENSO respond to paleo-climate change?
7. How does ENSO respond to global warming?
8. What processes lead to different ENSO "flavours"?

To raise awareness of the advances and the important outstanding issues amongst the next generation of climate scientists, the CLIVAR Pacific Panel organised a summer school on "ENSO: dynamics and predictability" for young aspiring international students. The lush jungles of Puna on the Big Island of Hawaii provided an ideal setting. This region is under the spell of ENSO, and is subject to the whims of the Hawaiian volcano goddess Pele. The summer school was located a mere 5 miles from where the active and spectacular Kilauea Lava flow spills into the ocean.

Sixteen outstanding students and 6 lecturers from 11 different countries participated. All students had a strong background in meteorology, oceanography or geology. The lecturers included 4 members of the CLIVAR Pacific Panel (Magdalena Balmaseda - ECMWF, Mike McPhaden- NOAA PMEL, Scott Power- Bureau of Meteorology and Axel Timmermann - IPRC), Fei-Fei Jin from the University of Hawaii and Richard Kleeman from the Courant Institute (NYU). Topics covered during 4 hours of daily lectures included ENSO theory (Fei-Fei Jin), ENSO phenomenology (Mike McPhaden), ENSO prediction (Magdalena Balmseda), paleo ENSO (Axel Timmermann), decadal changes in ENSO and the impact of global warming on ENSO (Scott Power) and ENSO predictability theory (Richard Kleeman). The lectures were complemented by challenging student research projects, evening presentations, field excursions to the Mauna Loa CO_2 observatory and the Volcano National Park. Energizing brain fuel consisted of fresh goat milk kefir, locally grown vegetables and fruits and freshly caught fish from the deep blue Pacific.

The research projects engaged the students in investigations of e.g.: the effect of multiplicative weather "noise" on ENSO variability and predictability; the impact of El Niño on Antarctic climate; evidence for the origin of a megadrought 4,200 years ago in existing hydrological paleo-data sets; the role of wave dynamics in the dynamics of ENSO using TAO-Triton data; the termination mechanism for the 2006-2008 ENSO event; and the nature of warm pool El Nino events. Students applied the concepts taught during the lectures to their research projects.

More details on the student projects as well as pdf-files for all lectures can be found on: http://iprc.soest.hawaii.edu/~axel/ENSOsummerschool.html

The summer school was generously supported by WCRP, PAGES, NOAA, ARCNESS, the Australian Bureau of Meteorology, the International Pacific Research Center and Mathworks.

Participants at the ENSO Summer School

Contents

Editorial	2
The Southwest Pacific Ocean Circulation and Climate Experiment (SPICE): a new CLIVAR programme	3
Evaulation of water masses in ocean syntheses products	7
On isothermal diagnostics of ocean heat content	9
The role of West African coastal upwelling in the genesis of tropical cyclones: a new mechanism	11
Madden–Julian oscillation forecasting at operational modelling centres	18
Numerical simulations of the role of land surface conditions on the climate of Mt. Kilimanjaro region	20
Quantifying climate–related risks and uncertainties ujsing Cox regression models	23
Report on the CLIVAR Pacific Panel Summer School on "ENSO: dynamics and predictability" in Puna, on the Big Island of Hawaii	27

The CLIVAR Newsletter Exchanges is published by the International CLIVAR Project Office
ISSN No: 1026 - 0471

Editors: Kate Stansfield and Howard Cattle
Layout: Sandy Grapes
Printing: Technart Limited, Southampton, United Kingdom

CLIVAR Exchanges is distributed free of charge upon request (email: icpo@noc.soton.ac.uk)

The ICPO is supported by the UK Natural Environment Research Council and NASA, NOAA and NSF through US CLIVAR.

If undelivered please return to:
International CLIVAR Project Office
National Oceanography Centre Southampton
University of Southampton Waterfront Campus
Southampton, SO14 3ZH, United Kingdom
http://www.clivar.org